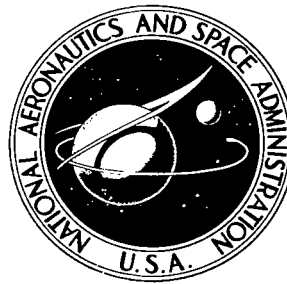


NASA TECHNICAL NOTE



NASA TN D-6307

C.1

NASA TN D-6307



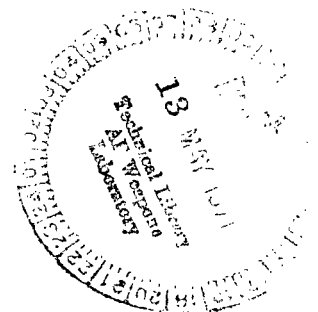
LOAN COPY: RETURN
AFWL (DOGL)
KIRTLAND AFB, N. M.

EFFECTS OF HIGH ACCELERATIONS AND HEAT FLUXES ON NUCLEATE BOILING OF WATER IN AN AXISYMMETRIC ROTATING BOILER

by Paul J. Marto and Vernon H. Gray

Lewis Research Center

Cleveland, Ohio 44135





0133109

1. Report No. NASA TN D-6307	2. Government Accession No.	3. Recipient
4. Title and Subtitle EFFECTS OF HIGH ACCELERATIONS AND HEAT FLUXES ON NUCLEATE BOILING OF WATER IN AN AXISYMMETRIC ROTATING BOILER		5. Report Date May 1971
7. Author(s) Paul J. Marto and Vernon H. Gray		6. Performing Organization Code
9. Performing Organization Name and Address Lewis Research Center National Aeronautics and Space Administration Cleveland, Ohio 44135		8. Performing Organization Report No. E-6040
12. Sponsoring Agency Name and Address National Aeronautics and Space Administration Washington, D. C. 20546		10. Work Unit No. 120-27
15. Supplementary Notes		11. Contract or Grant No.
16. Abstract <p>Stable boiling in a rotating cylindrical annulus with continuous through-flow of water was obtained at heat fluxes as high as 818 000 Btu/(hr)(ft²) (2.58 MW/m²) at atmospheric pressure. Incipient- and nucleate-boiling heat-transfer coefficients were obtained at accelerations up to 400 g's. Measurements were made of void fractions, radial temperature profiles, and wall pressures in the boiling fluid. Convective secondary-flow cells and fluid temperature inversions were revealed. Increased fluid thicknesses increased heat-transfer coefficients, but inlet liquid subcooling had no effect. Coefficients increased with acceleration at low heat fluxes, but at high fluxes varied less than the usual data scatter.</p>		13. Type of Report and Period Covered Technical Note
17. Key Words (Suggested by Author(s)) Boiling heat transfer Acceleration effects on boiling Rotating boiler		14. Sponsoring Agency Code
18. Distribution Statement Unclassified - unlimited		
19. Security Classif. (of this report) Unclassified	20. Security Classif. (of this page) Unclassified	21. No. of Pages 59
		22. Price* \$3.00

EFFECTS OF HIGH ACCELERATIONS AND HEAT FLUXES ON NUCLEATE BOILING OF WATER IN AN AXISYMMETRIC ROTATING BOILER

by Paul J. Marto* and Vernon H. Gray

Lewis Research Center

SUMMARY

Nucleate-boiling data were obtained using a heated-wall rotating boiler with continuous through-flow of water as the test fluid. The boiler was rotated at speeds up to 2660 rpm, giving radial accelerations up to 400 g's at the test surface. Heat fluxes as high as 818 000 Btu per hour per square foot (2.58 MW/m^2) were attained with stable boiling at atmospheric pressure. Radial temperature profiles in the two-phase boiling fluid were measured. Effects of aging of the test surface were noted; however, these effects diminished with time.

Visual observation of the boiling two-phase fluid annulus revealed secondary flow cell circulation which increased with acceleration and was also influenced by inlet liquid feed and by heat flux level. Bubble nucleation at the heated surface was sharply reduced at high accelerations with corresponding increases in local fluid subcoolings and decreases in measured average vapor void fractions in the fluid annulus. The inlet water subcooling had no measurable effect on boiling heat transfer, but heat-transfer coefficients were increased by increases in the thickness of the two-phase fluid annulus.

For the inception of nucleate boiling from natural convection, the heat flux and required wall superheat increased as the acceleration increased. For nucleate boiling, heat-transfer coefficients increased with acceleration at low heat fluxes but were practically independent of acceleration up to 400 g's at very high heat fluxes.

INTRODUCTION

In an effort to increase the stability and heat-flux capability of pool boilers and vapor generation devices, both in space and on Earth, the concept of a rotating boiler

*Assistant Professor of Mechanical Engineering, Naval Postgraduate School, Monterey, California; NASA Summer Faculty Fellow in 1968.

has been under study for several years at the Lewis Research Center (ref. 1). A small cylindrical copper boiler, 4.0 inches (10.2 cm) in diameter and 2.0 inches (5.1 cm) high, has been constructed. Reference 2 describes the operation of this boiler, presenting boiling heat-transfer coefficients at accelerations up to 200 g's. Photographic data up to 475 g's and a motion picture film supplement, which show the effects of rotation on boiling and liquid-vapor separation, are also included.

The nucleate-boiling heat-transfer results obtained in reference 2 showed a definite cross-over trend in the data, in which an increase in acceleration increased the heat-transfer coefficients at low heat fluxes but decreased them slightly at high heat fluxes. This trend agrees with the earlier data of Merte and Clark (ref. 3), which were taken at accelerations up to 20 g's. Both their data and the data of reference 2 were obtained using saturation temperatures at the boiler wall. These temperatures were not measured but were calculated using the estimated increase in hydrostatic pressure at the boiler wall due to acceleration. In the case of reference 2, however, this hydrostatic pressure increase was based upon the measured two-phase fluid annular thickness. The boiling fluid was assumed to be all liquid in the calculations because the true two-phase fluid density (or void fraction) was not known. This assumption of all liquid in the boiler resulted in an uncertainty in the converted experimental data, particularly at the higher accelerations and heat fluxes. In addition, the experimental results of reference 2 may have been influenced by variations in liquid inlet subcooling and boiler fluid level, which were not controlled during operation.

Effects of acceleration on nucleate boiling continue to be of interest, as evidenced by recent contributions to the heat-transfer literature. Pool-boiling heat-transfer coefficients in water were reported at accelerations up to 134 g's by Adelberg and Schwartz in reference 4. In their experiments, a container of water with a heater ribbon immersed in it was rotated on a centrifuge arm. Their results and the data of Costello and Tuthill (ref. 5) show that over the gravity range of 1 to 134 g's, gravity has an effect upon nucleate boiling only through the local variation in hydrostatic head at the test surface, and when the data are plotted using the saturation temperature at the boiler wall, all the data may be represented by a single curve with no cross-over trend. However, their data do show considerable scatter, and they point out that "one should not rule out the possibility of observing an effect of gravity upon nucleate boiling at sufficiently high g levels." Experimental pool-boiling data, obtained in a similar manner, using water and Arcton 11 (similar to Freon), were presented at accelerations to 65 g's by Turton in reference 6. His data are plotted using wall-to-bulk temperature differences, and he concludes that acceleration has little effect upon the temperature difference (and therefore heat-transfer coefficient) in nucleate boiling for heat fluxes up to 60 000 Btu per hour per square foot. Natural-convection and pool-boiling heat-transfer measurements using water in a 5.67-inch- (14.4-cm-) diameter by 1.0-inch- (2.5-cm-)

high centrifugal boiler were made at accelerations to 1280 g's by Eschweiler, Benton, and Preckshot (ref. 7). Their nucleate-boiling data show a strong influence of gravity in the natural-convection-influenced boiling region, but no conclusions can be made regarding a cross-over trend at higher heat fluxes.

The objectives of this investigation were therefore to obtain improved nucleate-boiling data for water in a rotating boiler with continuous through-flow of fluid by more accurately measuring the local temperature and surface hydrostatic pressure within the boiling fluid; to extend data on boiling heat-transfer coefficients to accelerations and heat fluxes higher than those reported in reference 2; and to study, within the limitations of the existing apparatus, the effects of fluid level and liquid inlet subcooling on the boiling heat-transfer variables.

EQUIPMENT AND CALIBRATIONS

The test apparatus is shown schematically in figure 1. It was the same apparatus as that described in reference 2, but with several modifications.

Description of Equipment

Liquid supply system. - Demineralized triple-distilled water was used in the experiments; this water was stored in the large stainless-steel supply tank shown in figure 1. The distilled water was pressure-fed through a porous metal filter and a micro-flow turbine-type flowmeter. Nitrogen gas was used to pressurize the tank. The feed lines were stainless-steel tubes with 3/8-inch (0.95-cm) outside diameter and were trace-heated with 1/4-inch (0.63-cm) copper steam lines and wrapped with asbestos strips.

An additional heat exchanger and storage tank were added subsequent to the reference 2 tests to control more closely the liquid inlet temperature to the rotating boiler. A 0.38-inch- (0.95-cm-) diameter stainless-steel helically wound coil, about 4.0 inches (10.2 cm) in diameter and 12.0 inches (30.5 cm) high was wrapped with 1.0-inch- (2.5-cm-) wide fiberglass-insulated electrical heating tape. The outlet line of this heat exchanger coil was connected to the top of a 3.0-inch- (7.6-cm-) diameter by 12.0-inch- (30.5-cm-) high stainless-steel storage vessel which was also electrically heated. The outlet line from this storage vessel was connected to the rotating face seal at the bottom of the hollow shaft (see fig. 1).

Test boiler. - The test boiler was a 4.0-inch- (10.2-cm-) inside-diameter copper cylinder, 2.0 inches (5.1 cm) high. It was mounted on a vertical shaft and was designed

to rotate at variable speeds up to 3000 rpm.

A cross section of the boiler is shown in figure 2. Liquid flowed upward inside the vertical shaft, passed through a regulating valve, and then sprayed out to the cylindrical walls, where it formed a liquid annulus. Feed liquid passed up into the heated zone through eight small holes (0.078 in. or 0.198 cm in diameter) to replace the fluid that boiled off. These feed holes were located tangential to the boiler test surface. Vapor produced in the boiling process separated from the fluid annulus (because of centrifugal force) and flowed out the top of the boiler along the axis of rotation. The thickness of the fluid annulus was controlled by the adjustable float-activated linkage to the regulating valve.

The boiler was heated by an 11-gage Chromel-A wire in a 3/16-inch- (0.47-cm-) outside-diameter Inconel sheath with alumina insulation. This heater was helically wound and furnace-brazed into a recess in the outside of the cylindrical copper boiler wall. Fiberglass insulation was packed around the float chamber and heater coils to reduce heat losses. The copper heat-transfer surface of the boiler was hot wiped with a layer of pure tin about 5 mils (0.13 mm) thick prior to the present tests.

Clear preshrunk plastic windows were installed in the annular region on top of the boiler so that the liquid-vapor interface and the boiling action could be observed. As shown in figure 2, two annular windows, 0.25 inch (0.63 cm) thick, were provided to allow accurate measurement of the liquid and two-phase fluid levels during operation. The design of these windows also permitted calculation of the average vapor void fraction in the two-phase fluid annulus. The bottom window contained three 0.031-inch- (0.079-cm-) diameter drilled holes tangential to the boiling test surface. These holes permitted liquid to flow up into the unheated, nonboiling, top annular space during operation.

The outlet vapor duct engaged a stationary felt rubbing seal in the 2-inch- (5.1-cm-) diameter pipe assembly leading to the condenser. The condenser was a cubical metal box open to the atmosphere at the bottom. Four nozzles sprayed cold tap water into the condenser box.

Instrumentation. - The boiling test instrumentation is shown schematically in figures 1 and 2. Four thermocouples rotated with the boiler. Six leads (for three thermocouples) were brought out of the rotating system through six silver sliprings at the top of the vapor space. Each silver slipring made contact with two spring-loaded silver-graphite brushes which were constructed to permit only momentary contact with the sliprings in an effort to reduce frictional heating. Because of facility limitations, the two leads for the fourth thermocouple were brought out of the rotating system through two less-accurate sliprings below the boiler.

The heated boiler wall thermocouple (T_w) was a single 26-gage constantan wire joined to the copper wall with solder at the end of a drilled hole 0.040 inch (0.102 cm)

in diameter, 1.0 inch (2.5 cm) up from the bottom of the heated cylinder, and 0.098 ± 0.002 inch (0.25 ± 0.005 cm) from the cylinder inside diameter. (All symbols are defined in the appendix.) The heated wall surface temperature was obtained by calculation with known values of the copper conductivity, the heat flux, and the thermocouple location. The other three rotating thermocouples were 30-gage, two-wire, copper-constantan, glass-insulated, metal-sheathed (0.062-in. or 0.16-cm od) assemblies with exposed ball junctions. The second rotating thermocouple ($T_{2\phi}$) measured the temperature of the two-phase boiling fluid at a point 0.13 inch (0.32 cm) radially inward from the heated wall surface and 1.0 inch (2.5 cm) up from the bottom. Provisions were also made to vary the radial position of this thermocouple while keeping it aligned circumferentially with the boiler wall thermocouple. The third rotating thermocouple ($T_{in,l}$) measured the temperature of the feed liquid about 0.12 inch (0.30 cm) from one of the inlets to the boiling test section. The fourth (less accurate) rotating thermocouple (T_l) measured the temperature of the nonboiling liquid in the annulus above the heated test section. The thermocouple voltages for these circuits were recorded using a high-precision digital voltmeter. Rotating thermocouple circuitry is shown in more detail in reference 2. The exit vapor temperature was measured by a stationary sheathed thermocouple mounted just above the sliprings.

A 1.0-pound-per-square-inch (6.9-kN/m^2) differential pressure transducer was connected to the top of the stationary outlet vapor container to record the pressure in the vapor space. Heat flow into the boiler was measured with a wattmeter calibrated to within ± 1.5 percent error.

Calibration Procedures

Heat-loss calibration. - To determine boiler heat losses, the inside of the boiler was packed with fiberglass insulation. The boiler was assembled exactly as for normal operation, but the water inlet valve was closed so that the boiler would be dry. Saturated steam from the 5-pound-per-square-inch- (35-kN/m^2 -) gage building steam line was introduced at the boiler outlet to maintain the top sliprings at the saturated steam temperature. The main heater was turned on, and the heat input was fixed at some low power level. The speed of the boiler was then varied at this power level. The system remained at each speed setting until thermal equilibrium was reached; the temperature of the heated-wall thermocouple was then recorded. At this equilibrium temperature, the amount of power put into the system was the same as that being lost. It was assumed that this power was the same as the heat lost from the boiler during normal boiling operation at this same equilibrium wall temperature and speed. By repeating the procedure for different heat inputs, the heat loss was obtained as a function of rotational

speed for various equilibrium temperatures. At 250° F (395 K) equilibrium temperature, the heat loss was never more than 135 watts. The calibrated heat loss was subtracted from the gross power input to obtain the actual heat flux through the test surface.

Pressure transducer calibration. - The pressure transducer was calibrated in place over the range of 0 to 1.0 pound per square inch (6.9 kN/m²) gage by varying a known height of water above the transducer from 0 to 27.8 inches (70.6 cm). At each water level setting above the transducer, the output voltage of the transducer was recorded on a digital voltmeter. The response of the transducer was linear with an output sensitivity of 0.35 millivolt per inch of water. During these tests, live steam at atmospheric pressure was introduced into the slipring vapor space to compensate for the transducer sensitivity to temperature.

Calibration of thermocouples. - Considerable care was exercised in calibrating the thermocouples. The entire outside of the boiler was packed with fiberglass insulation. Saturated steam from the 5-pound-per-square-inch- (35-kN/m²-) gage building steam line was introduced into the boiler through the feed water inlet. The steam flowed past the bottom thermocouple sliprings, through the boiler, past the top thermocouple sliprings, and out through the condenser. The stationary thermocouple in the vapor space was accurately checked by comparing its reading with the saturation temperature calculated from the measured pressure in the vapor space.

The boiler was then rotated, and the tension of the top slipring brushes was adjusted so that frictional heating effects at the slipring-brush junction were at a minimum level. (The tension of the bottom slipring brushes, for the nonboiling liquid annulus thermocouple, could not be regulated.) The top brushes were then moved away from their respective sliprings to avoid contact. The boiler speed was then successively set at 515, 660, 940, 1330, 1880, and 2660 rpm (corresponding to 15, 25, 50, 100, 200, and 400 g's at the heating surface, respectively). At each speed setting, the top brushes were placed against the sliprings, making contact momentarily. The momentary readings of the three rotating thermocouples using the top sliprings and the reading from the bottom sliprings were then compared with the reading of the stationary vapor space thermocouple. The deviation of each rotating thermocouple from saturation temperature in the vapor space was recorded at each speed setting. This procedure was repeated several times, and after each time the slipring assembly was dismantled and reassembled. Table I gives the calibration data for various speed settings giving the average of about six deviations of each thermocouple from the saturated vapor temperature calculated for the measured pressure. This average deviation was either subtracted from or added to each thermocouple reading during operation to arrive at a corrected thermocouple voltage (or temperature). For comparison purposes, for copper-constantan at 220° F (378 K), a change of 0.026 millivolt corresponds to 1° F (0.56 K).

Wall pressure and void fraction measurement. - During steady operation of the boiler, it is possible to measure both the pressure at the heated cylinder wall and the average vapor void fraction within the two-phase fluid annulus. As shown in figure 3, because of the design of the two top annular windows, liquid is allowed to flow through the connecting holes into the top annular space when the boiler is rotated. When heat is added to the boiler, two different annular thicknesses result: h in the nonboiling liquid and $h_{2\phi}$ in the two-phase mixture. The difference in these thicknesses is due to the difference in density between the two-phase mixture and the pure liquid. Consequently, the top annular space can be used as a differential manometer.

In addition, the pressure field within the fluid can be calculated using the fundamental equations of fluid mechanics which describe rotational motion. We simplify the fluid motion by assuming that in the two-phase annulus the secondary flow caused by bubble-induced convection, natural convection, and liquid feed into the boiler can be considered to be small and can therefore be neglected. In this case the fluid moves only in the tangential direction with no radial or axial velocity components. Thus, both the top liquid annulus and the bottom two-phase annulus are assumed to rotate as a solid body about the vertical axis with a uniform angular velocity ω .

Under these circumstances the pressure field varies with radial and axial position. The radial component of the pressure gradient becomes

$$\frac{\partial p}{\partial r} = \rho \frac{\omega^2 r}{g_0} \quad (1)$$

and the axial hydrostatic gradient is

$$\frac{\partial p}{\partial z} = -\rho \frac{g}{g_0} \quad (2)$$

These two equations may be integrated to obtain pressure variations in both the radial and axial directions.

Thus, at the test surface, $r = R$, we can obtain the following hydrostatic pressure variations from equation (2):

$$P_w = P_1 + \rho_{2\phi} \frac{g}{g_0} H \quad (3)$$

and

$$P_1 = P'_1 + \rho_l \frac{g}{g_0} H' \quad (4)$$

where $\rho_{2\varphi}$ is the average effective density of the two-phase mixture in the bottom annulus and ρ_l is the liquid density in the top, unheated annulus.

Similarly, equation (1) may be integrated to obtain the following pressure variations in the radial direction:

$$P_1 = P_v + \frac{\rho_{2\varphi} \omega^2}{2g_0} (R^2 - r_1^2) \quad (5)$$

and

$$P'_1 = P_{\text{atm}} + \frac{\rho_l \omega^2}{2g_0} (R^2 - r_1'^2) \quad (6)$$

or since

$$r_1 = R - h_{2\varphi}$$

and

$$r_1' = R - h$$

then equations (5) and (6) may be written as

$$P_1 = P_v + \frac{\rho_{2\varphi} \omega^2}{2g_0} h_{2\varphi} (2R - h_{2\varphi}) \quad (7)$$

$$P'_1 = P_{\text{atm}} + \frac{\rho_l \omega^2}{2g_0} h (2R - h) \quad (8)$$

Determination of wall pressure: The local pressure at the test surface wall may be obtained by first eliminating the two-phase density $\rho_{2\phi}$ from equation (3) by using equation (7). Therefore,

$$P_w = P_1 + \left[\frac{(P_1 - P_v)2g_o}{\omega^2 h_{2\phi}(2R - h_{2\phi})} \right] \frac{g}{g_o} H \quad (9)$$

or

$$P_w = P_v + (P_1 - P_v) \left[1 + \frac{\frac{2gH}{\omega^2}}{h_{2\phi}(2R - h_{2\phi})} \right] \quad (10)$$

Equations (4) and (8) are now successively substituted into equation (10) to get

$$P_w = P_v + \left[(P_{atm} - P_v) + \rho_l \frac{g}{g_o} H' + \frac{\rho_l \omega^2}{2g_o} h(2R - h) \right] \left[1 + \frac{\frac{2gH}{\omega^2}}{h_{2\phi}(2R - h_{2\phi})} \right] \quad (11)$$

Using this equation, the pressure at the test surface wall can be calculated, provided the pressures P_v and P_{atm} are measured, the speed N (equal to $30 \omega/\pi$) is measured, and the thicknesses h and $h_{2\phi}$ are measured.

Determination of average vapor void fraction: The average effective density in the two-phase annulus is defined as

$$\rho_{2\phi} = \alpha \rho_v + (1 - \alpha) \rho_L \quad (12)$$

where

α average vapor void fraction

ρ_v density of vapor

ρ_L density of liquid in heated annulus

Note that, because the top annulus is unheated, the liquid temperature there is less than the saturation temperature in the heated annulus. Hence, the liquid density in the top annulus ρ_l is not equal to the liquid density in the heated annulus ρ_L .

The void fraction becomes

$$\alpha = \frac{1 - \frac{\rho_{2\phi}}{\rho_L}}{1 - \frac{\rho_v}{\rho_L}} \quad (13)$$

and α can be determined by solving for the two-phase density $\rho_{2\phi}$ by using equations (4), (7), and (8) and substituting this result into equation (13). Equations (4) and (7) are set equal to one another to give

$$P_1' + \rho_l \frac{g}{g_0} H' = P_v + \frac{\rho_{2\phi} \omega^2}{2g_0} h_{2\phi} (2R - h_{2\phi}) \quad (14)$$

Equation (8) is then used to eliminate P_1' :

$$P_{atm} + \frac{\rho_l \omega^2}{2g_0} h(2R - h) + \rho_l \frac{g}{g_0} H' = P_v + \frac{\rho_{2\phi} \omega^2}{2g_0} h_{2\phi} (2R - h_{2\phi}) \quad (15)$$

Upon solving for $\rho_{2\phi}$, we obtain

$$\rho_{2\phi} = \frac{(P_{atm} - P_v)}{\frac{\omega^2 h_{2\phi} (2R - h_{2\phi})}{2g_0}} + \frac{\rho_l h(2R - h)}{h_{2\phi} (2R - h_{2\phi})} + \frac{\rho_l \frac{g}{g_0} H'}{\frac{\omega^2 h_{2\phi} (2R - h_{2\phi})}{2g_0}} \quad (16)$$

The average vapor void fraction α can be calculated by using equations (13) and (16), provided the pressures P_v and P_{atm} , the speed N , and the thicknesses h and $h_{2\phi}$ are measured.

Equation (16) may be put into a dimensionless form

$$\frac{\rho_{2\varphi}}{\rho_l} = \frac{h(2R - h)}{h_{2\varphi}(2R - h_{2\varphi})} \left[1 + \frac{(P_{atm} - P_v)}{\rho_l \omega^2 h(2R - h)} + \frac{\rho_l \frac{g}{g_o} H'}{\rho_l \omega^2 h(2R - h)} \right] \quad (17)$$

and if we define

$$\xi = \frac{h}{R}$$

$$\xi_{2\varphi} = \frac{h_{2\varphi}}{R}$$

and slightly rearrange equation (17) we get

$$\frac{\rho_{2\varphi}}{\rho_l} = \frac{\xi(2 - \xi)}{\xi_{2\varphi}(2 - \xi_{2\varphi})} \left[1 + \frac{2(P_{atm} - P_v)}{\rho_l \frac{\omega^2 R^2}{g_o} \xi(2 - \xi)} + \frac{2gh \frac{H'}{h}}{\omega^2 R^2 \xi(2 - \xi)} \right] \quad (18)$$

OPERATIONAL PROCEDURES

Testing procedures and chronology will be presented in some detail because boiling heat transfer is known to be affected by many subtle conditions of the test surface and fluid. Many times throughout the program the test surface was cleaned in an effort to control corrosion and pitting of the surface. A photograph showing some of this pitting is shown in figure 4. The surface was cleaned with cleansing powder using a cotton swab and water. Then it was thoroughly rinsed with distilled water and wiped with cotton saturated with a degreasing agent.

Except as noted later, the rotating boiler stood idle overnight prior to a test run and was allowed to fill with air when not operating. When two or more runs were made the same day, at least 1 hour elapsed between data points in successive runs. Prior to taking experimental data (1) the water in the supply tank and feed lines was electrically heated to a temperature near 175° F (352 K), (2) the supply tank was pressurized to about 30 pounds per square inch (207 kN/m²) gage with nitrogen, (3) the boiler was rotated with no heat input, (4) the water supply valve was opened to allow water flow into

the boiler, and (5) the power input to the boiler was gradually increased until boiling commenced. The system was operated under these conditions for about 30 minutes to degas the boiler surface. Upon shutdown the reverse sequence was followed.

The rotating boiler was operated for 15 runs, which comprised six major groupings, as outlined in table II. The data obtained are presented in chronological order in table III. Operational procedures for each group of these tests are given in the subsequent sections in the same order as listed in table II.

Reproducibility Tests

Runs 4, 5, and 6 (see table III) were made to evaluate the repeatability of rotating boiler data. During run 4 at 25 g's and run 6 at 200 g's, the speed of rotation was fixed and the power input was gradually increased from 500 to approximately 20 kilowatts, and then gradually decreased. Prior to run 4, the test surface was recleaned using the cleaning procedure described previously. In an effort to compare this recleaned test surface to an "aged" test surface, run 5 was made after the boiler had been operated during run 4 and after it had been standing for $1\frac{1}{2}$ hours. The operational procedure of run 5 was identical to that of run 4.

Subcooling

Runs 2 and 3 were made to study the effect of inlet water subcooling (saturation minus inlet temperature) on boiler operation at 25 and 200 g's, respectively. During these runs, the temperature at the inlet to the rotating boiler was regulated by electrically controlling the water temperature in the supply tank and feed lines. At each value of rotational speed and heat flux level, data were taken as the inlet temperature was raised from 143° to 189° F (335 to 360 K).

Fluid Level

Several runs were made to investigate the effect of fluid level on boiler heat transfer. The thickness of the two-phase fluid annulus in the boiler was varied by adjusting the float-regulated needle valve at the inlet to the boiler. As described in reference 2, this rotating float valve generally maintained the fluid level constant over large variations in both rotational speed and heat flux, although minor erratic variations did occur.

In run 7 (and also run 6) at 200 g's, the fluid level was arbitrarily fixed, and the heat flux was varied up to a maximum and then decreased. In runs 8, 9, and 10, the inlet water supply valve was closed after water was introduced and the fluid thickness reached approximately 0.75 inch (1.9 cm). With the power supply set at a fixed value, boiling occurred and the thickness of the two-phase fluid annulus decreased. Temperature data were taken as the fluid level decreased. During run 8 at 200 g's and runs 9 and 10 at 25 g's data were recorded at four or five levels as the thickness decreased. This procedure was repeated for several settings of power input.

Fluid Temperature Profiles

In run 13, the thickness of the two-phase fluid annulus was kept constant and the radial position of the rotating thermocouple in the fluid annulus was varied. In run 14, the radial position of the thermocouple was held fixed while the thickness of the fluid annulus was varied.

During run 13, the position of the local fluid thermocouple was set $1/32$ inch (0.079 cm) radially inward from the test surface after fixing its circumferential and axial positions. The boiler was then operated at 25 g's with a two-phase fluid thickness of approximately 0.41 inch (1.04 cm) and a total power input of 1.50 kilowatts. When thermal equilibrium was reached, a thermocouple reading was made. The power input was then shut off and the boiler rotation was stopped so that the radial position of the thermocouple could be altered without changing its circumferential or axial position. With a new radial position of the thermocouple, the procedure was repeated. Temperature data were taken with the thermocouple set at $1/16$ inch (1.59 cm) intervals from $1/32$ to $13/32$ inch (0.079 to 1.03 cm) radially inward from the boiler surface. Data were obtained at speeds of 25 and 200 g's and at total power inputs of 1.5 and 6.0 kilowatts.

During run 14, the boiler was operated at 400 g's with the water inlet supply valve closed, and with the local fluid thermocouple held fixed at $1/4$ inch (0.64 cm) from the test surface. The run started with a nonboiling liquid annulus thickness of 0.375 inch (0.952 cm) and a power input of 1.5 kilowatts. During operation, as the water was evaporated away, the thickness of the two-phase fluid annulus decreased. Temperature data were taken as the thickness of the top liquid annulus changed from 0.375 to 0.063 inch (0.952 to 0.159 cm). This procedure was repeated at a second power input level of 6.0 kilowatts.

Boiling Incipience

Runs 11 and 12 were made at low power inputs to obtain natural convection data and to observe the incipience of nucleate boiling for various rotative accelerations. During run 11 the speed of the boiler was successively fixed at 660, 940, 1330, 1880, and 2660 rpm (corresponding to 25, 50, 100, 200, and 400 g's at the heating surface, respectively). At each speed setting the total power input was gradually increased in steps of 150 watts from an initial value of 150 watts up to approximately 600 watts, by which value nucleate boiling generally had commenced. The operational procedure of run 12 was similar to run 11 except that the rotative acceleration was initially set at 400 g's and was successively decreased to 25 g's.

Nucleate Boiling

Two runs were made at inlet water subcoolings from approximately 20° to 55° F (11 to 30 K) to investigate the effects of acceleration on nucleate-boiling heat transfer. During run 1, the nominal power input was fixed at 500 watts, and the rotative acceleration was successively fixed at 15, 25, 50, 100, 200, and 400 g's. The power input was then increased, and the rotation was again varied in the same order. This procedure was repeated for six power levels to 9.0 kilowatts. During this run, the two-phase fluid level in the boiler varied between 0.188 and 0.656 inch (0.480 and 1.67 cm).

Run 15 was made with an approximately constant two-phase fluid level of 0.375 inch (0.95 cm). The nominal power input was fixed at 1.7 kilowatts, and the rotation was successively fixed at 50, 100, 200, and 400 g's. The power input was then increased, and the speeds were again varied in the same order. This procedure was repeated for eight power levels to 35 kilowatts. The boiler was then operated for several minutes at 400 g's with a power input of 42 kilowatts. A short circuit occurred in the main electrical heater before full data could be obtained.

RESULTS AND DISCUSSION

General

Performance characteristics. - Visual observation of the boiling process showed that the boiler operated in a steady manner with a stable liquid-vapor interface. For example, at 400 g's the boiler operated in a steady manner even at a total power input of 42 kilowatts, which is a radial heat flux of 818 000 Btu per hour per square foot. This

heat flux is estimated to be twice the critical, or "burnout" heat flux for atmospheric pool boiling of water at normal gravities.

The rotating boiler operated essentially at atmospheric pressure; its exit vapor space pressure was always within 1 inch (2.5 cm) of water of the ambient atmospheric pressure. For most of the runs (when the water supply valve was open), the boiler had an approximately constant inventory of liquid, but with a continuous throughflow whose rate depended on the power input. At low power inputs (low flows), the boiler inventory was large relative to the inflow, and pool boiling was simulated. On the other hand, at high power inputs, throughflow was larger and secondary-flow cells developed in the boiling annulus.

Figure 5 is a sketch showing the typical visual appearance of the boiling annulus at low and high accelerations for the same heat flux. At low accelerations there were many active nucleation sites on the boiling surface, giving rise to many large size bubbles in the boiling annulus. The fluid in the boiling annulus had a frothy appearance and the liquid-vapor interface of the annulus was quite irregular. In contrast to this irregular shape, the water in the top nonboiling annulus at all accelerations behaved as in solid body rotation, with a smooth mirror-like interface (see figure 5(a)). At high accelerations, the number of active sites was sharply reduced, and bubble sizes were smaller. Also, secondary-flow cells disrupted bubble nucleation, and the boiling annulus appeared as in figure 5(b). Normally the convection cells correlated in number and position with the liquid feed holes. The liquid-vapor interface was not as irregular at high accelerations as at low accelerations. Reference 2 discusses the effects of acceleration and power input on the boiling action, showing photographs and providing a motion-picture film supplement (C-253) which is available on loan.

Void fraction. - From observations of the liquid level h' in the nonboiling upper annulus and the two-phase fluid thickness $h'_{2\phi}$ in the boiler (see table III), the average vapor void fraction α in the two-phase boiling annulus can be calculated using equations (13) and (16). This average void fraction is plotted as a function of acceleration in figure 6 for three levels of heat flux. Data from reference 8 for nucleate pool boiling of water at 1 g and 1 atmosphere are also included.

Even though the uncertainty in these data is fairly large because of the difficulty in measuring the thickness of the two-phase fluid annulus, a definite trend can be observed. As the acceleration increases at a fixed heating rate, the average void fraction decreases. This shows there are fewer vapor voids in the boiling fluid, presumably because there are fewer active nucleation sites and also smaller size bubbles. This trend agrees with the results of Graham and Hendricks (ref. 9), who showed that both the number of active sites and the maximum bubble departure diameter decrease with increasing acceleration. It is also apparent in figure 6 that, at any given rotative speed, the void fraction increases with heat flux as expected.

Reproducibility and Aging

Runs 4, 5, and 6 were made specifically to check for repeatability of the nucleate-boiling data, effects (if any) of surface cleaning procedure, and effects of progressively increasing the heat flux compared with decreasing it (hysteresis). Within the data of these three runs, no consistent effects or conclusions could be determined. All the plots of wall temperature against heat flux data of runs 4 and 5 at 25 g's fell within a scatter band width of $\pm 1.5^{\circ}\text{F}$ ($\pm 0.8\text{ K}$). Run 6 (and also run 7) at 200 g's was similar except for the data at a heat flux near 116 000 Btu per hour per square foot ($365\,000\text{ W/m}^2$), which indicated that wall temperatures during a decrease from high boiling heat fluxes at high g's can be as much as 4°F (2.2 K) hotter than comparable values during the initial startup from low heat-flux levels. This could be a manifestation of outgassing and subsequent progressive flooding of smaller and smaller surface cavities (which slowly refill with air during down periods).

In review of all the data runs, a significant and reasonably consistent trend, herein labelled "aging," appeared. This trend is illustrated in figure 7 for increasing-heat-flux data taken at 200 g's. Figure 7 is a typical boiling heat-transfer plot, in which the heat flux normal to the test surface Q/A is plotted against the wall superheat $T_w - T_{\text{sat},w}$. The saturation temperature at the heated wall $T_{\text{sat},w}$ is determined from the saturation temperature curve for water for the pressure at the wall P_w calculated from equation (11). Figure 7 shows that, as running time elapsed, the wall superheat increased for the same heating level. Fortunately, this increase was much slower in the second half of the program than it was at first (between runs 1 and 6). Also, data taken during any one run or during consecutive runs are much less affected by this aging than would be indicated by the total spread of data in figure 7.

The cause of the surface aging effect could not be pinpointed. It is assumed to be the combined effects of surface pitting, corroding and scaling, and possibly the progressive flooding of smaller and smaller cavities with liquid.

Inlet Liquid Subcooling

The subcooling referred to here is the difference between the saturation temperature at the boiler wall and the temperature of the inlet liquid at the feed holes, $T_{\text{sat},w} - T_{\text{in},l} = \Delta T_{\text{sub}}$. The effect of inlet subcooling at 25 and 200 g's is shown in figure 8, wherein heat flux is plotted against wall superheat $T_w - T_{\text{sat},w}$. It is evident that inlet subcooling does not measurably affect the nucleate-boiling results. This result is consistent with subcooled, forced flow, fully developed boiling data of reference 10, taken with water at 1 g and low pressures. It is concluded, therefore, that

inlet subcooling, even at high accelerations, is not important in studying nucleate-boiling data of Q/A as a function of $T_w - T_{sat,w}$. Consequently, the data of reference 2 should be applicable in this respect, even though inlet subcooling was not independently regulated.

Fluid Level

The effect of five different levels of fluid in the boiling annulus (measured in the top nonboiling annulus), with no inlet feed supply, is shown in figure 9 for both 200 and 25 g's. As the thickness of the fluid annulus increases (with a corresponding increase in pressure at the heated wall), the wall superheat decreases. This decrease, at a given heat flux, is an increase in boiling heat-transfer coefficient (presented in table III) and is in agreement with the well-known pressure effect in pool boiling (ref. 11). Whether or not other effects are present, such as increased convection velocities with increased fluid thicknesses, cannot be determined from the data.

Fluid Temperature Profiles

In reference 2, temperatures in the two-phase rotating annulus were measured at only one point, 1/8 inch (0.32 cm) radially inward from the heated wall. On the basis of this limited amount of data, fluid temperature "inversions" were postulated to exist in the boiling annulus (fig. 17 of ref. 2). In the present investigation, the local fluid temperature was measured at several distances from the wall along a radial line in the horizontal midplane of the boiler, as shown in figure 10.

The two-phase fluid temperatures, obtained in run 13, are shown in figure 11 for heat fluxes near 27 000 and 115 000 Btu per hour per square foot (85 000 and 362 000 W/m^2) at accelerations of 25 and 200 g's. It is evident that a distinct temperature inversion exists inward from the heated thermal sublayer. Also it appears that the fluid bulk temperature is generally less than the saturation temperature in the vapor (and of course less than the calculated local saturation temperature in the fluid, $T_{sat,f}$). Furthermore, the degree of local subcooling appears to increase with an increase in acceleration. This local subcooling is also evident in figure 12, which shows the local fluid temperature measured at a constant position 1/4 inch (0.64 cm) from the test surface for the two heat fluxes and 400 g's during run 14, in which the water feed supply was valved off. Note that, when the thermocouple is within the fluid annulus, the temperature reads considerably less than vapor saturation (as much as 9.6° F (5.3 K) less), and when the liquid-vapor interface passes over the thermocouple, leaving it in the vapor space.

readings near the saturation temperature are obtained. (For run 14, the liquid-vapor interface is estimated to be 1/32 inch (0.08 cm) radially inward from the measured nonboiling liquid interface in the top annulus.)

The results presented in figures 11 and 12 may appear contrary to the rule that during bulk boiling, with net evaporation, the average fluid bulk temperature must be slightly superheated. This apparent contradiction may be explained when it is realized that the local fluid thermocouple measured the radial temperature profile at only one circumferential and axial position. This radial profile position may not have been representative of the whole boiling annulus, as will be discussed next.

Referring again to figure 10, during the boiling process subcooled water enters the boiler through feed holes at the outer radius at the bottom of the test surface. This colder, denser liquid is centrifuged radially outward and flows both circumferentially and axially upward to form an annulus of colder liquid just inward from the heated thermal sublayer on the wall. However, this annulus is observed to be broken up by the bubbles leaving the surface, and convective secondary-flow cells are formed in the horizontal plane, as mentioned earlier and shown at the top of figure 10. It is possible that the local fluid thermocouple measured radial temperature profiles mainly in the cooler outward-bound leg of a convective cell, as illustrated. Superimposed on this flow, in a vertical plane through the axis, a tertiary-flow cell, or "smoke-ring" torous, is postulated, as shown at the bottom of figure 10. The resultant of these motions is a complex swirling flow in the boiler; probing this fluid annulus to obtain an accurate average bulk temperature would be very difficult.

It is also possible that the volume-averaged fluid bulk temperature is in fact subcooled, as figures 11 and 12 would indicate. At least once, in run 15, data point 24, the secondary cells travelled circumferentially around the boiler and past the feed holes. In this case the local fluid thermocouple must have measured the circumferential-average fluid temperature 4/32 inch (0.32 cm) radially inward from the heated surface; this temperature was subcooled 4.8°F (2.7 K) below the vapor temperature $T_{\text{sat},v}$. In any case, the conventional fluid bulk temperature is not obtainable from these data. Instead, the calculated saturation temperature at the wall $T_{\text{sat},w}$ is used herein to present the heat-transfer data.

Natural-Convection to Nucleate-Boiling Incipience

The effect of acceleration on natural convection and incipient boiling is shown in figure 13 using the data of runs 11 and 12. The incipient boiling point is defined as that heat flux at which bubble formation is first observed. As noted earlier, the data of run 11 were taken for increasing speed while the data of run 12 were taken for decreas-

ing speed. The test surface was precleaned prior to each run, and the fluid levels were approximately the same. The agreement between the data presented in runs 11 and 12 is good. Note that in each case, as the gravity level increases, the heat transfer increases for a given temperature difference, as expected. In addition, the incipient boiling data confirm the results of Graham and Hendricks (ref. 9) that, as the acceleration increases, both heat flux and wall superheat increase at incipient boiling.

Figure 14 shows the natural-convection data at or near boiling incipience plotted conventionally as Nusselt number Nu as a function of the product of Grashof number Gr and Prandtl number Pr . The correlation of Fishenden and Saunders (ref. 12) for natural convection from a horizontal plate is given for comparison, even though a large uncertainty in the experimental data exists in this low heat flux region, and the temperature difference in the Grashof and Nusselt numbers involves $T_w - T_{sat,w}$ rather than $T_w - T_{bulk}$, as discussed earlier.

Nucleate Boiling

Because of the surface aging factors previously discussed, and the fact that the fluid level was not maintained constant during run 1, the nucleate-boiling data of run 15 are considered superior to those of run 1. In figure 15, heat flux from run 15 is plotted against wall superheat $T_w - T_{sat,w}$ for accelerations of 50, 100, 200, and 400 g's. In the low-heat-flux boiling region (where natural convection is important), the boiling coefficient increases markedly as acceleration increases; values of this coefficient (ratio of ordinate to abscissa) are given in table III. The coefficient increases as much as 60 percent from 50 to 400 g's.

At the higher heat fluxes the heat-transfer curves for the various accelerations converge into a narrow band of wall superheat values ($\pm 2^{\circ} F$; $\pm 1 K$), with the higher accelerations converging at progressively higher heat fluxes. Within the narrow band of wall superheats at high heat fluxes, a slight trend is evident for a reversal of the effect of acceleration compared with that at low heat fluxes. Such a reversal, with its necessary "cross-over" region, has been reported and discussed before (refs. 2 to 7), and in view of the present data with their more accurate wall saturation pressures, is still debatable. Adelberg and Schwartz (ref. 4) conclude similarly, after analyzing the previously available nucleate-boiling data at high accelerations. Shown in figure 16 are selected data at high accelerations from the present report and from reference 2, compared with the band of data given in reference 4. The NASA data (herein and ref. 2) fall along the center of this band and extend to much higher heat fluxes and accelerations. Thus, the major effects of acceleration on nucleate boiling are portrayed in figure 16,

and any "reversal" at high heat fluxes is as small in magnitude as the usual scatter in experimental data.

SUMMARY OF RESULTS

Using an axisymmetric rotating boiler with an electrically heated cylindrical wall and continuous throughflow of water as test fluid, the following principal results were obtained:

1. Stable nucleate-boiling heat-transfer data at atmospheric pressure were obtained at radial accelerations up to 400 g's and at heat fluxes up to 818 000 Btu per hour per square foot (2.58 MW/m^2).
2. The following effects of acceleration were observed in the data as rotative accelerations increased:
 - a. Boiling-heat-transfer coefficients increased at low heat fluxes (as much as 60 percent in going from 50 to 400 g's); at very high heat fluxes the coefficients were practically independent of acceleration.
 - b. Bubble nucleation and average vapor void fractions in the boiling annulus decreased, at constant heating levels.
 - c. Convective secondary-flow cells increased in vigor and separated the boiling fluid annulus into alternating zones of bubbly and relatively clear liquid.
 - d. Fluid temperature profiles developed steeper radial gradients, with increased local temperature inversions below saturated vapor temperature (as much as 9.6° F or 5.3 K).
 - e. Natural-convection to nucleate-boiling incipency occurred at progressively higher heat fluxes and higher wall superheats.
3. Inlet water subcooling had no measurable effect on boiling heat transfer, but increases in fluid thickness in the boiling annulus increased the boiling heat-transfer coefficients (especially at high acceleration and low heat flux).
4. The heat-transfer surface "aged" during the elapsed time of the runs, requiring gradually increased wall superheats for a given heat flux; this effect diminished with time.

Lewis Research Center,
National Aeronautics and Space Administration,
Cleveland, Ohio, January 6, 1971,
120-27.

APPENDIX - SYMBOLS

A	area, ft^2 ; m^2	k	thermal conductivity of liquid, $\text{Btu}/(\text{hr})(\text{ft})(^{\circ}\text{F})$; $\text{W}/(\text{m})(\text{K})$
a/g	ratio of rotational acceleration to acceleration of gravity	N	rotational speed of boiler, rpm
c_p	specific heat of liquid, $\text{Btu}/(\text{lbm})(^{\circ}\text{F})$; $(\text{W})(\text{sec})/(\text{g})(\text{K})$	Nu	Nusselt number, $h_{\text{NC}} D/k$
D	characteristic dimension in natural convection correlation equal to \sqrt{A} , ft; m	P	pressure, lb/ft^2 abs; N/m^2
Gr	Grashof number, $\beta(T_w - T_{\text{sat}, w})g D^3/\nu^2$	Δp	pressure rise across two-phase fluid annulus, $\text{lb}/\text{in.}^2$; N/m^2
g	acceleration due to gravity, $32.2 \text{ ft}/\text{sec}^2$; $9.8 \text{ m}/\text{sec}^2$	P_{atm}	atmospheric pressure, lb/ft^2 abs; N/m^2
g_0	$32.2 \text{ ft-lbm}/(\text{lb})(\text{sec}^2)$; $1 \text{ m-Kg}/(\text{N})(\text{sec}^2)$	P_v	pressure in vapor space, lb/ft^2 abs; N/m^2
H	one-half of vertical height of boiler, ft; m	P_w	pressure at midpoint of heated surface; lb/ft^2 abs; N/m^2
H'	vertical distance from top of boiler wall to midpoint of top unheated annulus, ft; m	P_1	pressure at top of heated surface, lb/ft^2 abs; N/m^2
h	thickness of top nonboiling liquid annulus, ft; m	P_1'	pressure at midpoint of top unheated surface, lb/ft^2 abs; N/m^2
h'	thickness of top nonboiling liquid annulus, in.; cm	Pr	Prandtl number, $\mu c_p/k$
h_{NC}	natural-convection heat-transfer coefficient, $\text{Btu}/(\text{hr})(\text{ft}^2)(^{\circ}\text{F})$; $\text{W}/(\text{m}^2)(\text{K})$	Q/A	heat flux, $\text{Btu}/(\text{hr})(\text{ft}^2)$; W/m^2
$h_{2\phi}$	thickness of two-phase fluid annulus, ft; m	R	radius of heated wall, ft; m
$h_{2\phi}'$	thickness of two-phase fluid annulus, in; cm	r	radial position, ft; m
		r_1	radius of interface of two-phase annulus, ft; m
		r_1'	radius of interface of top liquid annulus, ft; m
		T	temperature, $^{\circ}\text{F}$; K

T_{bulk}	bulk temperature of liquid, $^{\circ}\text{F}; \text{K}$	β	volume coefficient of expansion, $^{\circ}\text{F}^{-1}; \text{K}^{-1}$
$T_{\text{in}, l}$	temperature of inlet liquid, $^{\circ}\text{F}; \text{K}$	μ	absolute viscosity of liquid, $\text{lbm}/(\text{ft})(\text{hr}); \text{kg}/(\text{m})(\text{sec})$
T_l	temperature of nonboiling liquid annulus, $^{\circ}\text{F}; \text{K}$	ν	kinematic viscosity of liquid, $\text{ft}^2/\text{sec}; \text{m}^2/\text{sec}$
$T_{\text{sat}, \text{atm}}$	saturation temperature at atmospheric pressure, $^{\circ}\text{F}; \text{K}$	ξ	dimensionless ratio, h/R
$T_{\text{sat}, f}$	saturation temperature in fluid annulus, $^{\circ}\text{F}; \text{K}$	$\xi_{2\phi}$	dimensionless ratio, $h_{2\phi}/R$
$T_{\text{sat}, v}$	saturation temperature in vapor space, $^{\circ}\text{F}; \text{K}$	ρ	density, $\text{lbm}/\text{ft}^3; \text{kg}/\text{m}^3$
$T_{\text{sat}, w}$	saturation temperature at boiler wall, $^{\circ}\text{F}; \text{K}$	ρ_L	density of liquid in heated annulus, $\text{lbm}/\text{ft}^3;$ kg/m^3
ΔT_{sub}	liquid inlet subcooling, $T_{\text{sat}, w} - T_{\text{in}, l}, ^{\circ}\text{F}; \text{K}$	ρ_l	density of liquid in top unheat- ed annulus, $\text{lbm}/\text{ft}^3;$ kg/m^3
T_W	boiler wall surface tempera- ture, $^{\circ}\text{F}; \text{K}$	ρ_v	density of vapor, $\text{lbm}/\text{ft}^3;$ kg/m^3
z	vertical position, ft; m	$\rho_{2\phi}$	effective density in two-phase fluid annulus, $\text{lbm}/\text{ft}^3;$ kg/m^3
α	average void fraction in boiling fluid	ω	angular velocity of boiler, rad/sec

REFERENCES

1. Gray, Vernon H.: Feasibility Study of a Rotating Boiler for High-Performance Rankine Cycle Power Generation Systems. *Advances in Energy Conversion Engineering*. ASME, 1967, pp. 145-149.
2. Gray, Vernon H.; Marto, Paul J.; and Joslyn, Allan W.: Boiling Heat Transfer Coefficients, Interface Behavior, and Vapor Quality in a Rotating Boiler Operating to 475 G's. NASA TN D-4136, 1968.
3. Merte, Herman, Jr.; and Clark, J. A.: Pool Boiling in an Accelerating System. *J. Heat Transfer*, vol. 83, no. 3, Aug. 1961, pp. 233-242.
4. Adelberg, Marvin; and Schwartz, S. H.: Nucleate Pool Boiling at High G Levels. *Chem. Eng. Progr. Symp. Ser.*, vol. 64, no. 82, 1968, pp. 3-11.
5. Costello, C. P.; and Tuthill, W. E.: Effects of Acceleration on Nucleate Pool Boiling. *Chem. Eng. Progr. Symp. Ser.*, vol. 57, no. 32, 1961, pp. 189-196.
6. Turton, J. S.: The Effects of Pressure and Acceleration on the Pool Boiling of Water and Arcton 11. *Int. J. Heat Mass Transfer*, vol. 11, no. 9, Sept. 1968, pp. 1295-1310.
7. Eschweiler, James C.; Benton, Allan M.; and Preckshot, George W.: Boiling and Convective Heat Transfer at High Accelerations. *Chem. Eng. Progr. Symp. Ser.*, vol. 63, no. 79, 1967, pp. 66-72.
8. Iida, Yoshihiro; and Kobayasi, Kiyosi: Distributions of Void Fraction above a Horizontal Heating Surface in Pool Boiling. *JSME Bull.*, vol. 12, no. 50, Apr. 1969, pp. 283-290.
9. Graham, Robert W.; and Hendricks, Robert C.: A Study of the Effect of Multi-G Accelerations on Nucleate-Boiling Ebullition. NASA TN D-1196, 1963.
10. Jeglic, Frank A.; Stone, James R.; and Gray, Vernon H.: Experimental Study of Subcooled Nucleate Boiling of Water Flowing in 1/4-Inch-Diameter Tubes at Low Pressures. NASA TN D-2626, 1965.
11. McAdams, William H.: *Heat Transmission*. Second ed., McGraw-Hill Book Co., Inc., 1942.
12. Fishenden, M.; and Saunders, O. A.: *An Introduction to Heat Transfer*. Clarendon Press, Oxford, 1950.

TABLE I. - THERMOCOUPLE CALIBRATION DATA

($\pm 0.026 \text{ mV} = \pm 1^\circ \text{ F}$ (0.56 K) at 220° F (378 K).)

Thermocouple location	515 rpm	660 rpm	940 rpm	1330 rpm	1880 rpm	2660 rpm
	Average deviation ^a , mV					
Boiler wall (differential)	-0.008 ± 0.004	-0.013 ± 0.006	-0.025 ± 0.012	-0.011 ± 0.006	-0.015 ± 0.005	-0.013 ± 0.003
Two-phase fluid	-0.001 ± 0.005	-0.014 ± 0.008	-0.013 ± 0.003	-0.015 ± 0.007	-0.015 ± 0.007	-0.012 ± 0.005
Inlet liquid	0.039 ± 0.018	0.040 ± 0.022	0.037 ± 0.018	0.027 ± 0.015	0.029 ± 0.012	0.031 ± 0.015
Top nonboiling liquid ^b	-0.01 ± 0.04	-0.03 ± 0.04	-0.07 ± 0.06	-0.09 ± 0.06	-0.11 ± 0.07	-0.17 ± 0.01
Outlet vapor (nonrotating)	0.013 ± 0.004	0.013 ± 0.005	0.013 ± 0.003	0.013 ± 0.002	0.013 ± 0.002	0.012 ± 0.002

^aThermocouple reading minus saturation temperature based on pressure in vapor.

^bThis thermocouple output was more erratic than other thermocouple outputs because lower sliprings were not as accurate as top sliprings, and momentary readings could not be taken.

TABLE II. - GROUPING OF EXPERIMENTAL RUNS

Group	Chrono-logical run number	Operating mode	Test surface preparation	Run operating time, hr	Cumulative operating time, hr
Reproducibility	4	At 25 g's. vary heat flux to a maximum, then decrease it.	Precleaned and pre-boiled	1.0	18.0
	^a 5	At 25 g's. vary heat flux to a maximum, then decrease it.	Preboiled, not pre-cleaned	1.0	19.0
	6	At 200 g's. vary heat flux to a maximum, then decrease it.	Preboiled, not pre-cleaned	1.5	20.5
Subcooling	2	At 25 g's and at fixed heat fluxes, vary liquid inlet temperature.	Not pre-cleaned, not preboiled	4.0	13.0
	3	At 200 g's and at fixed heat fluxes, vary liquid inlet temperature.	Not pre-cleaned, not preboiled	4.0	17.0
Fluid level	^a 7	At 200 g's and fixed fluid level, vary heat flux.	Preboiled, not pre-cleaned	1.0	21.5
	^a 8	At 200 g's and fixed heat fluxes, take data with water supply valve closed.	No changes from run 7	1.0	22.5
	9	At 25 g's and fixed heat fluxes, take data with water supply valve closed.	No changes from run 8	2.0	24.5
	^a 10	At 25 g's and fixed heat fluxes, take data with water supply valve closed.	Precleaned and pre-boiled	2.0	26.5
Fluid temperature profiles	13	For 25 and 200 g's at fixed heat fluxes, vary position of fluid annulus thermocouple.	No changes from run 12	2.5	35.5
	^a 14	At 400 g's, fixed heat flux, and no inlet feed, read fluid annulus thermocouple.	No changes from run 13	1.5	37.0
Boiling incipience	11	At fixed speeds (increasing), vary power input from 150 to 600 W.	Precleaned and pre-boiled	3.5	30.0
	^a 12	At fixed speeds (decreasing), vary power input from 150 to 600 W.	Precleaned and pre-boiled	3.0	33.0
Nucleate boiling	1	At fixed heat fluxes (increasing), vary speed from 15 to 400 g's.	Precleaned, not pre-boiled	9.0	9.0
	15	At fixed heat fluxes (increasing), vary speed from 50 to 400 g's.	Precleaned and pre-boiled	5.5	42.5

^aOperated same day as preceding run.

TABLE III. - EXPERIMENTAL DATA

(a) U. S. Customary Units

Run	Data point	Rotational acceleration, a, g	Heat flux, Q, A , Btu (hr)(ft ²)	Vapor exit saturation temperature, $T_{sat, V}$, °F	Liquid flow rate, lb/hr	Two-phase fluid annulus thickness, h'_{2o} , in.	Non-boiling liquid annulus thickness, h' , in.	Pressure rise across fluid annulus, Δp , psi	Wall surface saturation temperature, $T_{sat, W}$, °F	Wall surface temperature, T_W , °F	Local two-phase fluid temperature, T_{2o} , °F	Liquid inlet temperature, $T_{in, l}$, °F	Boiling heat-transfer coefficient, h , Btu (hr)(ft ²)(°F)	Remarks
1	2	15	10 150	210.7	----	0.188	0.063	0.06	210.9	226.4	209.1	169.3	654	
	3	25	10 150	↓	----	.250	.188	.20	211.4	226.7	208.4	169.8	662	
	4	50	10 000	↓	----	.313	.250	.45	212.3	227.7	206.4	170.5	650	
	5	100	9 780	↓	----	.344	.313	1.02	214.2	227.8	206.2	172.6	718	
	7	200	9 480	↓	----	.350	.328	2.10	217.7	229.5	203.8	176.6	802	
	8	400	9 100	210.4	----	.438	.406	5.20	226.6	234.2	199.9	184.5	1195	
	9	15	33 600	210.7	----	.344	.219	.15	211.2	231.4	209.1	169.3	1665	
	10	25	33 600	↓	----	.438	.344	.30	211.7	232.1	209.1	171.9	1645	
	11	50	33 400	↓	----	.469	.406	.65	213.0	233.7	208.5	174.2	1615	
	12	100	33 200	↓	----	.516	.469	1.47	215.7	235.2	207.4	175.6	1700	
	13	200	32 900	↓	----	.469	.438	2.76	219.7	237.7	205.9	179.4	1830	
	14	400	32 500	↓	----	.406	.375	4.80	225.7	241.8	200.0	188.2	2020	
	15	15	57 000	210.7	10.5	.406	.250	.16	211.3	235.3	209.1	169.0	2370	
	16	25	57 000	↓	↓	.406	.219?	.22	211.5	236.6	209.1	170.8	2270	
	17	50	56 800	↓	↓	.531	.438	.70	213.3	238.3	209.1	172.6	2270	
	18	100	56 700	↓	↓	.531	.469	1.47	215.7	239.9	207.9	176.4	2340	
	19	200	56 400	210.6	↓	.506	.484	3.0	220.3	243.1	205.6	178.8	2470	
	20	400	56 000	210.6	↓	.469	.453	5.7	228.2	248.9	203.7	185.2	2710	
	21	15	115 600	210.6	21	.484	.281	.18	211.3	239.1	209.4	167.9	4160	
	22	25	115 600	↓	↓	.438	.344	.31	211.6	240.1	209.4	168.9	4050	
	23	50	115 500	↓	↓	.500	.438	.70	213.2	242.5	208.4	169.7	3940	
	24	100	115 300	↓	↓	.563	.500	1.55	215.8	243.6	208.3	174.8	4150	
	25	200	115 100	↓	↓	.531	.500	3.1	220.6	248.0	206.1	179.1	4210	
	26	400	114 700	↓	↓	.438	.406	5.2	226.8	253.0	204.9	186.1	4380	
	27	15	176 000	210.6	31	.594	.438	.23	211.4	242.2	209.6	169.1	5720	
	28	25	↓	↓	↓	.594	.500	.41	212.0	243.2	209.7	169.9	5640	
	29	50	↓	↓	↓	.625	.563	.86	213.6	245.1	208.4	172.5	5590	
	30	100	↓	↓	↓	.656	.594	1.80	216.6	247.1	207.7	177.3	5770	
	31	200	↓	↓	↓	.625	.594	3.60	222.1	251.7	207.2	182.1	5940	
	32	400	↓	↓	↓	.531	.500	6.20	229.4	259.1	205.2	190.9	5930	
2	1	25	10 150	210.7	----	0.250	0.188	0.20	211.4	230.4	208.7	150.2	535	
	2	25	10 150	210.7	----	.250	.188	.20	211.4	229.8	208.8	170.9	552	
	3	25	10 150	210.7	----	.250	.188	.20	211.4	229.5	-----	181.9	561	
	4	25	33 600	210.7	----	.281	.181	.20	211.4	235.0	-----	143.7	1425	
	5	↓	↓	210.7	----	↓	.181	↓	211.4	235.0	-----	155.4	1425	
	6	↓	↓	210.7	----	↓	.188	↓	211.4	235.3	-----	168.2	1405	
	7	↓	↓	210.6	----	↓	.181	↓	211.3	235.5	-----	176.2	1390	
	8	25	68 800	210.5	13	.281	.163	.19	211.1	238.2	-----	143.6	2540	
	9	↓	↓	210.6	↓	↓	.172	↓	211.2	238.3	-----	155.8	2540	
	10	↓	↓	210.5	↓	↓	.172	↓	211.1	238.5	-----	169.5	2510	
	11	↓	↓	210.5	↓	↓	.172	↓	211.1	238.7	-----	180.5	2490	

TABLE III. - Continued. EXPERIMENTAL DATA

(a) Continued. U. S. Customary Units

Run	Data point	Rotative acceleration, a/g	Heat flux, Q/A Btu (hr)(ft ²)	Vapor exit saturation temperature, T _{sat, V} , °F	Liquid flow rate, lb/hr	Two-phase fluid annulus thickness, h _{2φ} , in.	Non-boiling liquid annulus thickness, h', in.	Pressure rise across fluid annulus, Δp, psi	Wall surface saturation temperature, T _{sat, W} , °F	Wall surface temperature, T _W , °F	Local two-phase fluid temperature, T _{2φ} , °F	Liquid inlet temperature, T _{in, l} , °F	Boiling heat-transfer coefficient, Q A(T _W - T _{sat, W}) Btu (hr)(ft ²)(°F)	Remarks
3	1	200	9 500	210.7	--	0.344	0.331	2.16	217.8	227.8	206.2	165.1	950	
	2	↓	↓	↓	--	.344	.331	↓	↓	228.0	206.2	174.9	932	
	3	↓	↓	↓	--	.344	.334	↓	↓	228.2	206.5	178.4	915	
	4	↓	↓	↓	--	---	---	↓	↓	228.4	206.1	186.4	897	
	5	200	32 900	210.7	--	.344	.328	2.15	217.7	237.6	207.5	163.7	1655	
	6	↓	↓	210.7	--	↓	↓	↓	217.7	237.8	207.3	167.5	1640	
	7	↓	↓	210.7	--	↓	↓	↓	217.7	238.0	207.2	170.6	1625	
	8	↓	↓	210.6	--	↓	↓	↓	217.6	237.3	207.2	179.6	1670	
	9	200	68 700	210.7	12	.359	.328	2.15	217.7	244.7	208.0	158.9	2550	
	10	↓	↓	210.7	↓	↓	↓	↓	217.7	244.5	208.0	166.4	2565	
	11	↓	↓	210.6	↓	↓	↓	↓	217.6	244.5	208.0	174.0	2555	
	12	↓	↓	210.6	↓	↓	↓	↓	217.6	244.3	208.3	182.4	2570	
	13	200	115 200	210.6	21	.359	.319	2.10	217.6	249.8	207.3	165.0	3580	
	14	200	115 200	210.6	21	.359	.319	2.10	217.6	249.9	208.7	170.4	3570	
	15	200	115 200	210.6	21	.359	.319	2.10	217.6	249.9	208.2	189.0	3570	
4	1	25	10 200	210.8	--	0.438	0.344	0.30	211.8	229.3	208.2	150.6	583	
	2	↓	33 600	↓	--	.281	.156	.17	211.4	237.9	208.4	163.0	1265	
	3	↓	57 200	↓	10	.313	↓	↓	↓	239.8	208.7	164.8	2015	
	4	↓	116 000	↓	22	↓	↓	↓	↓	243.0	209.4	163.5	3695	
	5	↓	176 000	↓	33	↓	↓	↓	↓	246.6	209.9	165.2	5000	
	6	↓	233 000	210.9	43	↓	↓	↓	211.5	249.8	210.2	169.3	6080	
	7	↓	355 000	210.9	64	↓	↓	↓	211.5	255.5	210.7	172.4	8060	
	8	↓	174 000	210.9	33	.281	↓	↓	211.5	248.9	210.2	174.5	4650	
	9	↓	118 000	210.8	23	↓	↓	↓	211.4	243.0	210.0	174.8	3730	
	10	↓	60 000	210.9	11	↓	.172	.18	211.5	238.5	209.5	175.4	2220	
	11	↓	34 000	210.9	--	↓	.178	.18	211.5	236.3	208.8	176.1	1370	
	12	↓	10 200	210.9	--	↓	.194	.20	211.5	230.5	207.5	177.2	537	
5	13	25	10 200	210.9	--	0.266	0.172	0.18	211.5	229.6	207.4	182.8	563	
	14	↓	34 000	↓	--	.281	.166	.18	↓	236.9	208.8	180.0	1340	
	15	↓	70 000	↓	13	.281	.163	.17	↓	240.9	209.2	176.5	2380	
	16	↓	141 000	↓	26	.281	.156	.17	↓	245.9	209.7	172.9	4100	
	17	↓	210 000	210.8	39	.297	.156	.17	211.4	250.2	209.9	172.8	5410	
	18	↓	300 000	↓	55	.313	.150	.16	↓	254.6	210.2	174.4	6950	
	19	↓	180 000	↓	33	.313	.156	.17	↓	247.7	209.7	176.2	4960	
	20	↓	93 500	↓	18	.297	.156	.17	↓	242.3	209.5	176.8	3025	
	21	↓	33 600	↓	--	.313	.188	.20	↓	236.8	208.2	178.4	1320	

TABLE III. - Continued. EXPERIMENTAL DATA

(a) Continued. U. S. Customary Units

Run	Data point	Rota- tive acceler- ation, a g	Heat flux, Q/A Btu (hr)(ft ²)	Vapor exit satura- tion tempera- ture, T _{sat, V} , °F	Liquid flow rate, lb/hr	Two- phase fluid annulus thickness, h' ₂ , in.	Non- boiling liquid annulus thickness, h', in.	Pressure rise across fluid annulus, Δp, psi	Wall surface satura- tion tempera- ture, T _{sat, W} , °F	Wall surface tempera- ture, T _W , °F		Local two- phase fluid tempera- ture, T _{2φ} , °F	Liquid inlet tempera- ture, T _{in, l} , °F	Boiling heat- transfer coefficient, Q A(T _W - T _{sat, W}) average, Btu (hr)(ft ²)(°F)	Remarks
										High	Low				
6	1	200	9 370	210.8	--	0.313	0.297	1.95	217.3	229.6	228.6	204.8	177.9	795	Boiling interrupted prior to point
	2		33 000	210.8	--	.313	.297	1.95	217.3	240.1	239.3	206.4	176.3	1470	
	3		57 600	210.9	11	.328	.297	1.95	217.4	245.7	243.9	207.2	184.4	2100	
	4		116 000	210.8	22	.328	.291	1.90	217.1	252.8	252.1	208.0	183.1	3280	
	5		176 000	210.8	33	.344	.288	1.90	217.1	257.0	256.5	208.1	183.2	4440	
	6		237 000	210.8	44	.359	.284	1.90	217.1	260.1	259.8	208.8	186.1	5530	
	7		350 000	210.9	64	-----	.272	1.80	216.9	265.2	264.9	208.9	188.9	7260	
	8		473 000	210.9	83	-----	.219	1.50	215.8	269.3	269.1	208.4	190.7	8860	
	9		237 000	210.8	45	.344	.281	1.85	216.9	261.4	260.8	207.0	191.4	5330	
	10		116 000	210.8	22	.344	.288	1.90	217.1	256.8	256.0	207.9	190.8	2950	
	11		57 600	210.6	11	.328	.294	1.95	217.0	246.7	245.8	205.5	190.1	1970	
	12		32 900	210.6	--	-----	-----	1.95	217.1	239.7	239.2	-----	185.8	1470	
	13		8 300	210.9	--	.313	.297	1.95	217.4	228.0	227.7	205.5	187.0	794	
	14		115 500	210.8	21	.344	.291	1.90	217.1	256.2	255.5	207.7	178.8	2980	
	15		116 000	210.8	21	.344	.288	1.90	217.1	256.3	255.1	208.2	171.4	3010	
7	1	200	33 000	211.0	--	-----	0.625	3.72	222.7	244.6	243.2	204.7	176.3	1555	Boiling interrupted prior to point
	2		57 000	211.0	11	-----	.531	3.25	221.4	247.9	245.9	205.3	183.0	2235	
	3		117 300	210.9	25	-----	.500	3.10	220.9	256.8	256.3	206.9	181.2	3290	
	4		175 000	211.0	35	0.469	.438	2.76	219.9	260.3	259.5	206.7	178.0	4370	
	5		238 000		44	.453	.406	2.60	219.4	262.6	261.9	207.6	179.8	5550	
	6		351 000		64	-----	.359	2.31	218.5	266.2	265.7	208.2	182.4	7400	
	7		235 000		44	.469	.438	2.76	219.9	263.4	262.8	206.7	184.9	5440	
	8		116 500		21	-----	.547	3.30	221.5	258.7	257.7	206.8	192.5	3180	
	9		56 500		10	-----	.719	4.15	224.0	250.4	245.4	204.4	188.5	2370	

TABLE III. - Continued. EXPERIMENTAL DATA

(a) Continued. U. S. Customary Units

Run	Data point	Rotative acceleration, g	Heat flux, Q A Btu $(hr)(ft^2)$	Vapor exit saturation temperature, $T_{sat}, V, ^\circ F$	Liquid flow rate, lb, hr	Two-phase fluid annulus thickness, $h'_{2\phi}, in.$	Non-boiling liquid annulus thickness, $h', in.$	Pressure rise across fluid annulus, $\Delta p, psi$	Wall surface saturation temperature, $T_{sat}, W, ^\circ F$	Wall surface temperature, $T_W, ^\circ F$		Local two-phase fluid temperature, $T_{2\phi}, ^\circ F$	Liquid inlet temperature, $T_{in}, ^\circ F$	Boiling heat-transfer coefficient, $Q A(T_W - T_{sat}, W)$ average, Btu $(hr)(ft^2)(^\circ F)$	Remarks
										High	Low	High	Low		
8	1	200	33 000	210.8	0	--	0.500	3.10	220.8	240.7	239.1	204.8	202.6	1730	Feed system
	2	200	33 000	210.8	0	--	.375	2.41	218.7	240.3	239.1	205.8	204.0	1570	valved off
	3	200	33 000	210.8	0	--	.250	1.67	216.4	238.8	238.4	205.4	204.3	1485	↓
	4	200	56 700	210.8	0	--	.625	3.72	222.5	249.6	247.2	205.8	203.8	2190	↓
	5	↓	↓	↓	↓	--	.500	3.10	220.8	249.2	247.2	206.0	203.7	2070	↓
	6	↓	↓	↓	↓	--	.375	2.41	218.7	248.4	247.1	206.1	204.6	1955	↓
	7	↓	↓	↓	↓	--	.250	1.67	216.4	247.3	246.5	207.0	206.0	1860	↓
	8	↓	↓	↓	↓	--	.219	1.48	215.8	248.2	247.5	207.7	206.8	1770	↓
	9	↓	↓	↓	↓	--	---	---	---	---	---	---	---	---	Feed system
	10	200	86 000	210.8	0	--	.500	3.10	220.8	254.6	253.8	206.2	---	2580	valved off
	11	↓	↓	↓	↓	--	.375	2.41	218.7	253.6	253.4	---	---	2470	↓
	12	↓	↓	↓	↓	--	.250	1.67	216.4	252.6	252.0	207.7	---	2400	↓
	13	↓	↓	↓	↓	--	.188	1.30	215.2	251.7	251.2	207.6	---	2370	↓
	14	200	115 500	210.8	0	--	.500	3.10	220.8	257.9	257.3	---	---	3140	Feed system
	15	↓	↓	↓	↓	--	.375	2.41	218.7	256.7	256.0	---	---	3070	valved off
	16	↓	↓	↓	↓	--	.250	1.67	216.4	254.8	254.5	---	---	3020	↓
	17	↓	↓	↓	↓	--	.188	1.30	215.2	253.5	253.2	---	---	3030	↓
9	1	25	10 150	211.0	0	--	0.500	0.42	212.4	229.9	229.3	209.0	207.8	590	Feed system
	2	↓	↓	211.1	↓	--	.375	.34	212.2	230.1	229.8	208.5	207.6	572	valved off
	3	↓	↓	211.0	↓	--	.250	.25	211.8	230.2	230.0	208.0	207.8	555	↓
	4	↓	↓	210.9	↓	--	.125	.15	211.5	231.1	230.9	207.3	206.5	520	↓
	5	↓	↓	---	↓	--	.063	.10	211.3	232.8	232.3	208.6	207.0	478	↓
	6	25	33 600	210.9	0	--	.500	.42	212.3	237.4	236.7	209.7	208.6	1355	Feed system
	7	↓	↓	210.9	↓	--	.375	.34	212.1	237.2	236.5	208.9	208.7	1355	valved off
	8	↓	↓	---	↓	--	.250	.25	211.7	237.4	236.7	208.7	208.3	1325	↓
	9	↓	↓	---	↓	--	.125	.15	211.4	237.9	237.3	208.8	208.4	1280	↓
	10	↓	↓	211.0	↓	--	.063	.10	211.3	238.3	238.1	210.7	210.6	1250	↓
	11	25	33 600	210.8	0	--	.375	.34	212.0	237.2	236.6	208.9	208.5	1350	Feed system
	12	↓	↓	210.8	↓	--	.250	.25	211.6	237.4	236.8	---	---	1315	valved off
	13	↓	↓	210.7	↓	--	.125	.15	211.2	237.6	237.1	208.4	208.0	1285	↓
	14	↓	↓	210.7	↓	--	.063	.10	211.0	238.1	237.8	210.7	210.5	1245	↓
	15	25	57 000	210.9	0	--	.500	.42	212.3	240.9	240.6	209.4	208.2	2005	Feed system
	16	↓	↓	210.8	↓	--	.375	.34	212.0	241.1	239.8	---	---	2005	valved off
	17	↓	↓	210.8	↓	--	.250	.25	211.6	240.6	240.3	208.7	208.3	1975	↓
	18	↓	↓	---	↓	--	.125	.15	211.3	240.8	240.6	---	---	1940	↓
	19	↓	↓	---	↓	--	.063	.10	211.1	240.4	240.3	---	---	1950	↓
	20	25	86 200	210.8	0	--	.500	.42	212.2	244.4	243.1	209.0	208.6	2730	Feed system
	21	↓	↓	↓	↓	--	.375	.34	212.0	243.7	243.4	---	---	2730	valved off
	22	↓	↓	↓	↓	--	.250	.25	211.6	244.0	243.8	---	---	2670	↓
	23	↓	↓	↓	↓	--	.125	.15	211.3	243.5	243.3	---	---	2690	↓
	24	↓	↓	↓	↓	--	.063	.10	211.1	243.5	243.3	---	---	2670	↓
	25	25	117 000	210.8	0	--	.500	.42	212.2	246.9	246.7	---	---	3380	Feed system
	26	↓	↓	↓	↓	--	.375	.34	212.0	246.7	246.6	---	---	3375	valved off
	27	↓	↓	↓	↓	--	.250	.25	211.6	246.4	246.3	---	---	3370	↓
	28	↓	↓	↓	↓	--	.125	.15	211.3	246.2	246.0	---	---	3360	↓
	29	↓	↓	↓	↓	--	.063	.10	211.1	245.9	245.8	---	---	3370	↓

TABLE III. - Continued. EXPERIMENTAL DATA

(a) Continued. U. S. Customary Units

Run	Data point	Rota- tive acceler- ation, a/g	Heat flux, Q/A Btu (hr)(ft ²)	Vapor exit satura- tion tempera- ture, T _{sat} , V, °F	Liquid flow rate, lb/hr	Two- phase fluid annulus thickness, h _{2φ} , in.	Non- boiling liquid annulus thickness, h', in.	Pressure rise across fluid annulus, Δp, psi	Wall surface satura- tion tempera- ture, T _{sat} , W, °F	Wall surface tempera- ture, T _W , °F		Local two-phase fluid tempera- ture, T _{2φ} , °F		Liquid inlet tempera- ture, T _{in} , l', °F	Boiling heat- transfer coefficient, Q A(T _W - T _{sat} , W) average, Btu (hr)(ft ²)(°F)	Remarks
										High	Low	High	Low			
10	1	25	10 150	210.8	0	-----	0.500	0.42	212.2	228.8	228.3	207.9	207.2	-----	621	Feed system
	2	↓	↓	210.6	↓	-----	.375	.34	211.8	229.6	228.9	208.2	207.6	-----	582	valved off
	3	↓	↓	210.5	↓	-----	.250	.25	211.3	229.2	229.0	208.0	207.8	-----	571	↓
	4	↓	↓	210.6	↓	-----	.125	.15	211.1	230.3	230.1	208.0	207.7	-----	532	↓
	5	↓	↓	210.6	↓	-----	.063	.10	210.9	231.3	231.1	210.6	-----	500	↓	
	6	25	33 600	210.7	0	-----	.500	.42	212.1	236.3	235.6	209.4	208.4	-----	1405	Feed system
	7	↓	↓	↓	↓	-----	.375	.34	211.9	235.6	235.2	208.4	207.7	-----	1430	valved off
	8	↓	↓	↓	↓	-----	.250	.25	211.5	236.9	236.5	208.7	207.8	-----	1330	↓
	9	↓	↓	↓	↓	-----	.125	.15	211.2	237.3	237.1	-----	-----	1290	↓	
	10	↓	↓	↓	↓	-----	.063	.10	211.0	237.5	237.4	209.2	208.9	-----	1270	↓
	11	25	57 000	210.7	0	-----	.500	.42	212.1	240.7	239.9	209.2	208.9	-----	2020	Feed system
	12	↓	↓	210.7	↓	-----	.375	.34	211.9	239.8	238.8	208.9	208.1	-----	2080	valved off
	13	↓	↓	210.6	↓	-----	.250	.25	211.4	240.0	239.7	209.0	208.7	-----	2000	↓
	14	↓	↓	210.6	↓	-----	.125	.15	211.1	240.1	239.9	-----	-----	1970	↓	
	15	↓	↓	210.6	↓	-----	.063	.10	210.9	240.9	240.8	-----	-----	1905	↓	
	16	25	89 400	210.5	0	-----	.500	.42	211.9	243.3	242.8	-----	-----	2870	Feed system	
	17	↓	↓	↓	↓	-----	.375	.33	211.7	242.9	242.7	-----	-----	2875	valved off	
	18	↓	↓	↓	↓	-----	.250	.25	211.3	242.7	242.4	-----	-----	2860	↓	
	19	↓	↓	↓	↓	-----	.125	.15	211.0	242.6	242.5	-----	-----	2830	↓	
	20	↓	↓	↓	↓	-----	.063	.10	210.8	242.6	242.5	-----	-----	2815	↓	
	21	25	116 000	210.6	0	-----	.500	.42	212.0	244.3	244.2	-----	-----	3600	Feed system	
	22	↓	↓	↓	↓	-----	.375	.34	211.8	244.2	244.0	-----	-----	3590	valved off	
	23	↓	↓	↓	↓	-----	.250	.25	211.4	244.4	244.2	-----	-----	3530	↓	
	24	↓	↓	↓	↓	-----	.125	.15	211.1	244.2	244.1	-----	-----	3510	↓	
	25	↓	↓	↓	↓	-----	.063	.10	210.9	244.8	244.6	-----	-----	3430	↓	
	26	↓	57 000	210.7	--	-----	.172	.19	211.3	240.4	240.3	208.8	208.6	-----	1960	Feed resumed
11	1	25	1 370	210.0	--	-----	0.328	0.30	211.1	218.7	218.6	208.3	208.0	157.5	182	Boiling
	2	↓	4 300	209.9	--	-----	.328	.30	211.0	222.9	222.8	207.4	207.1	163.6	363	↓
	3	↓	10 150	210.0	--	0.328	.281	.27	211.0	229.0	228.8	206.8	206.5	167.1	567	↓
	4	↓	1 370	209.8	--	.297	.281	.27	210.8	218.8	218.8	208.3	208.0	169.4	171	↓
	5	50	1 170	210.1	--	-----	.328	.55	212.0	221.0	220.9	207.7	207.1	172.8	131	Boiling
	6	↓	4 100	210.0	--	.313	.297	.51	211.8	223.2	223.1	206.8	206.3	173.5	361	↓
	7	↓	10 000	209.7	--	.297	.281	.49	211.4	228.7	228.4	206.9	206.5	175.3	583	↓
	8	↓	1 170	209.9	--	-----	.297	.51	211.7	218.6	218.5	207.8	207.5	174.7	171	↓
	9	100	977	209.9	--	-----	.344	1.12	213.8	221.3	221.2	206.4	206.0	175.9	131	Boiling
	10	↓	3 910	210.0	--	-----	.328	1.07	213.7	224.2	223.9	205.9	205.5	177.6	377	↓
	11	↓	9 770	210.1	--	.344	.313	1.02	213.6	229.2	229.1	206.4	205.7	178.1	628	↓
	12	↓	977	210.2	--	-----	.344	1.12	214.1	221.0	220.9	206.4	205.7	175.0	143	↓
	13	200	685	210.0	--	-----	.375	2.41	218.0	220.3	220.2	205.2	204.7	172.7	---	Natural convection
	14	↓	3 610	210.1	--	-----	.344	2.25	217.6	226.2	225.6	203.2	202.5	174.1	435	Boiling
	15	↓	6 550	210.1	--	-----	.338	2.20	217.4	226.6	226.3	203.8	203.1	177.3	724	Boiling
	16	↓	9 470	210.0	--	-----	.334	2.19	217.3	230.5	230.5	204.6	204.4	180.2	717	Boiling
	17	↓	685	209.9	--	-----	.359	2.32	217.6	219.4	219.2	205.5	205.3	174.4	---	Natural convection
	18	400	292	210.0	--	-----	.388	4.95	225.5	217.2	217.1	206.6	206.4	171.6	---	Natural convection
	19	↓	3 200	209.9	--	-----	.375	4.80	225.0	224.4	224.3	202.4	201.8	171.9	---	Natural convection
	20	↓	6 160	↓	--	-----	.375	4.80	225.0	230.3	230.2	199.1	198.5	173.4	---	Natural convection
	21	↓	9 100	↓	--	-----	.359	4.62	224.5	233.2	233.0	198.4	197.6	175.0	989	Boiling
	22	↓	15 000	↓	--	-----	.359	4.62	224.5	238.1	237.6	199.8	196.8	176.0	1125	Boiling

TABLE III. - Continued. EXPERIMENTAL DATA

(a) Continued. U. S. Customary Units

Run	Data point	Rotative acceleration, a/g	Heat flux, Q/A Btu (hr)(ft ²)	Vapor exit saturation temperature, T _{sat, V} , °F	Liquid flow rate, lb/hr	Two-phase fluid annulus thickness, h' _{2φ} , in.	Non-boiling liquid annulus thickness, h', in.	Pressure rise across fluid annulus, Δp, psi	Wall surface saturation temperature, T _{sat, W} , °F	Wall surface temperature, T _W , °F	Local two-phase fluid temperature, T _{2φ} , °F	Liquid inlet temperature, T _{in, l} , °F	Boiling heat transfer coefficient, Q A(T _W - T _{sat, W}) average, Btu (hr)(ft ²)(°F)	Remarks		
										High	Low					
12	1	400	292	209.8	-----	-----	0.375	4.80	224.9	214.3	214.2	207.6	207.2	160.3	----	Natural convection
	2	↓	3 200	209.7	-----	-----	.363	4.65	224.4	219.9	219.8	203.2	202.6	163.8	----	Natural convection
	3		6 160	209.9	-----	-----	.359	4.62	224.5	228.4	228.3	199.9	199.5	166.0	----	Natural convection
	4		9 100	209.8	-----	-----	.359	4.62	224.4	233.5	232.6	200.3	198.9	169.1	1050	Boiling
	5		15 000	209.7	-----	-----	.359	4.62	224.3	236.3	236.0	202.3	200.3	170.6	1265	Boiling
	6	↓	292	209.6	-----	-----	.366	4.68	224.4	215.2	215.1	207.0	206.4	167.6	----	Natural convection
	7	200	683	209.7	-----	-----	.400	2.55	218.1	218.0	217.8	205.4	205.0	168.3	----	Natural convection
	8	↓	3 620	209.6	-----	-----	.375	2.41	217.6	225.3	225.1	205.4	204.1	169.3	477	Boiling
	9		6 550	209.6	-----	-----	.350	2.28	217.2	226.8	226.6	205.2	204.8	172.4	690	Boiling
	10	↓	9 470	209.6	-----	-----	.334	2.19	216.9	228.3	228.1	204.9	203.3	175.3	838	Boiling
	11	100	976	209.7	-----	-----	.375	1.22	213.9	219.4	219.3	206.6	206.1	171.8	179	Boiling
	12	100	3 900	209.7	-----	-----	.341	1.11	213.5	222.9	222.1	205.6	205.2	174.2	433	Boiling
	13	100	9 760	209.7	-----	-----	.328	1.07	213.4	227.7	227.5	204.8	204.0	176.3	687	Boiling
	14	50	1 172	209.6	-----	-----	.313	.53	211.5	219.5	219.3	206.7	206.1	176.4	148	Boiling
	15	50	4 100	209.7	-----	-----	.297	.51	211.5	224.7	224.6	205.8	205.5	177.8	312	Boiling
	16	50	9 960	209.7	-----	-----	.281	.49	211.4	229.3	229.1	206.3	205.9	177.8	560	Boiling
	17	25	1 370	209.7	-----	-----	.250	.25	210.6	219.8	219.7	207.9	207.6	179.7	150	Boiling
	18	25	4 300	209.7	-----	-----	.225	.23	210.5	223.5	223.4	206.8	205.6	182.0	332	Boiling
	19	25	10 150	209.7	-----	-----	.203	.21	210.4	228.8	228.6	207.2	206.2	182.1	555	Boiling

TABLE III. - Continued. EXPERIMENTAL DATA

(a) Continued. U. S. Customary Units

Run	Data point	Rotative acceleration, a_g	Heat flux, Q/A Btu (hr)(ft ²)	Vapor exit saturation temperature, $T_{sat, V}$ °F	Liquid flow rate, lb/hr	Two-phase fluid annulus thickness, $h_{2\phi}$, in.	Non-boiling liquid annulus thickness, h' , in.	Pressure rise across fluid annulus, Δp , psi	Wall surface saturation temperature, $T_{sat, W}$ °F	Wall surface temperature, T_W °F	Local two-phase fluid temperature, $T_{2\phi}$ °F		Distance from wall of local two-phase fluid TC, in.	Liquid inlet temperature, $T_{in, l}$ °F	Boiling heat-transfer coefficient, $Q/A(T_W - T_{sat, W})$ Btu (hr)(ft ²)(°F)	Remarks
											High	Low				
13	1	25	27 800	210.3	---	---	0.313	0.30	211.3	233.0	206.6	205.9	1 32	153.5	1280	
	2	↓	↓	210.4	---	---	.328	↓	211.4	232.8	208.7	208.1	3 32	161.7	1300	
	3	↓	↓	210.4	---	---	.313	↓	211.4	232.0	209.3	208.5	5 32	171.1	1350	
	4	↓	↓	210.3	---	---	↓	↓	211.3	232.5	210.2	210.0	7 32	172.0	1310	
	5	↓	↓	210.0	---	---	↓	↓	211.0	232.3	210.6	210.3	9 32	175.0	1305	
	6	↓	↓	210.0	---	---	↓	↓	211.0	231.9	209.9	209.7	11 32	179.5	1330	
	7	↓	↓	210.0	---	---	↓	↓	211.0	232.4	210.2	210.0	13 32	178.3	1300	
	8	↓	↓	209.9	---	---	↓	↓	210.9	232.6	206.8	206.2	2 32	181.8	1280	
	9	25	116 000	209.9	---	---	.172	.18	210.5	245.0	206.6	206.1	1 32	176.4	3360	
	10	↓	↓	210.0	---	---	↓	↓	210.6	245.1	208.1	207.6	3 32	178.0	3360	
	11	↓	↓	210.0	---	---	↓	↓	210.6	245.3	209.2	209.0	5 32	180.3	3340	
	12	↓	↓	210.0	---	---	↓	↓	210.6	245.4	209.5	209.3	7 32	178.0	3330	
	13	↓	↓	209.9	---	---	↓	↓	210.5	245.0	210.0	210.0	9 32	178.2	3360	
	14	↓	↓	209.9	---	---	↓	↓	210.5	245.1	209.7	209.6	10 32	179.8	3350	
	15	200	27 100	209.9	---	---	.344	2.25	217.4	235.9	204.5	203.5	1 32	180.1	1465	
	16	↓	↓	209.8	---	---	.344	2.25	217.3	236.8	204.2	202.7	3 32	180.4	1390	
	17	↓	↓	209.7	---	---	.328	2.15	216.9	236.8	205.5	204.3	5 32	181.2	1365	
	18	↓	↓	209.8	---	---	↓	↓	217.0	236.5	205.3	204.1	7 32	181.8	1390	
	19	↓	↓	209.7	---	---	↓	↓	216.9	236.7	206.0	205.1	9 32	180.7	1370	
	20	↓	↓	209.8	---	---	↓	↓	217.0	236.5	206.6	206.4	11 32	181.8	1390	
	21	↓	↓	209.9	---	---	↓	↓	217.1	235.9	210.0	209.8	13 32	181.9	1440	
	22	↓	↓	210.0	---	---	↓	↓	217.2	235.6	209.4	208.4	12 32	181.1	1470	
	23	200	115 000	210.1	---	---	.328	2.15	217.3	252.3	206.4	203.4	1 32	175.8	3290	
	24	↓	↓	210.1	---	---	↓	↓	217.3	252.4	206.2	202.9	3 32	174.8	3280	
	25	↓	↓	210.0	---	---	↓	↓	217.2	252.0	207.6	205.6	5 32	175.0	3300	
	26	↓	↓	209.9	---	---	↓	↓	217.1	252.8	207.3	205.9	7 32	174.0	3230	
	27	↓	↓	209.8	---	---	↓	↓	217.0	252.2	207.9	206.7	9 32	176.0	3270	
	28	↓	↓	209.8	---	---	↓	↓	217.0	252.8	208.7	207.5	11 32	176.5	3220	
	29	↓	↓	209.8	---	---	↓	↓	217.0	252.1	209.9	209.5	13 32	178.2	3280	

TABLE III. - Continued. EXPERIMENTAL DATA

(a) Continued. U. S. Customary Units

Run	Data point	Rotative acceleration, a g	Heat flux, $\frac{Q}{A}$ $\frac{Btu}{(hr)(ft^2)}$	Vapor exit saturation temperature, $T_{sat, V}$ °F	Liquid flow rate, lb, hr	Two-phase fluid annulus thickness, h'_{2p} in.	Non-boiling liquid annulus thickness, h' in.	Pressure rise across fluid annulus, Δp , psi	Wall surface saturation temperature, $T_{sat, W}$ °F	Wall surface temperature, T_W	Local two-phase fluid temperature, T_{2p} °F		Distance from wall of local two-phase fluid TC, in.	Liquid inlet temperature, $T_{in, l}$ °F	Boiling heat-transfer coefficient, $\frac{Q}{A(T_W - T_{sat, W})}$ $\frac{3tu}{(hr)(ft^2)(^{\circ}F)}$	Remarks
											High	Low				
14	1	400	26 800	209.7	0	---	0.375	4.80	224.8	239.7	200.6	200.1	8.32	176.3	1800	Feed system
	2					---	.344	4.44	223.7	-----	201.4	200.4		180.3	-----	valved off
	3					---	.313	4.07	222.7	-----	203.0	202.0		-----	-----	
	4					---	.281	3.70	221.6	238.0	203.4	202.1		-----	1640	
	5			209.9		---	.250	3.30	220.7	-----	205.4	204.9		-----	-----	
	6					---	.219	2.92	219.5	-----	209.7	209.5		-----	-----	
	7					---	.188	2.55	218.3	-----	210.3	210.1		-----	-----	
	8					---	.156	2.16	217.2	-----	210.4	210.2		-----	-----	
	9					---	.125	1.75	215.8	-----	210.5	210.3		-----	-----	
	10					---	.094	1.35	214.6	237.1	210.4	210.2		-----	1190	
	11					---	.063	.92	213.1	-----	210.4	-----		-----	-----	
	16	400	115 000	210.0	0	---	.313	4.07	223.0	257.7	205.5	204.5	8.32	167.8	3320	Points 12 to 15
	17					---	.250	3.30	220.8	-----	206.3	205.2		-----	-----	unreliable; re-
	18					---	.188	2.55	218.4	-----	210.2	209.9		-----	-----	peated as 16 to
	19					---	.125	1.75	215.9	-----	210.4	210.3		-----	-----	20; Feed sys-
	20					---	.063	.92	213.2	-----	210.3	210.2		-----	-----	tem valved off

TABLE III. - Continued. EXPERIMENTAL DATA

(a) Concluded. U. S. Customary Units

Run	Data point	Relative acceleration, a/g	Heat flux, Q/A Btu (hr)(ft ²)	Vapor exit saturation temperature, $T_{sat, V}$ °F	Liquid flow rate, lb/hr	Two-phase fluid annulus thickness, $h'_{2\phi}$ in.	Non-boiling liquid annulus thickness, h' in.	Pressure rise across fluid annulus, Δp psi	Wall surface saturation temperature, $T_{sat, W}$ °F	Wall surface temperature, T_W °F	Local two-phase fluid temperature, $T_{2\phi}$ °F	Liquid inlet temperature, $T_{in, l}$ °F	Boiling heat-transfer coefficient, $Q/A(T_W - T_{sat, W})$ average, Btu (hr)(ft ²)(°F)	Remarks
15	1	50	33 400	210.4	---	0.344	0.281	0.49	212.2	241.8	241.5	154.8	1 135	Secondary cells rotating faster than boiler
	2	100	33 200	210.4	---	.406	.313	1.02	213.9	241.4	240.9	162.7	1 215	
	3	200	33 100	210.2	---	.375	.338	2.20	217.6	241.2	240.3	165.9	1 430	
	4	400	32 700	210.3	---	.375	.356	4.57	224.7	243.0	242.6	171.8	1 810	
	5	50	56 000	210.3	---	.344	.281	.49	212.1	243.6	243.1	161.5	1 790	
	6	100	54 300	210.3	---	.359	.313	1.02	213.8	245.4	244.8	162.8	1 735	
	7	200	54 100	210.2	---	.359	.338	2.20	217.6	246.4	245.9	166.2	1 895	
	8	400	53 700	209.9	---	.375	.350	4.50	224.1	247.7	245.7	169.9	2 380	
	9	50	116 500	210.0	21	.344	.281	.49	211.8	249.3	248.9	160.6	3 120	
	10	100	115 500	210.2	↓	.359	.316	1.02	213.8	250.9	250.6	163.6	3 120	
	11	200	115 000	209.9	↓	.359	.341	2.22	217.3	254.8	254.2	167.0	3 090	
	12	400	114 500	209.7	↓	.375	.344	4.43	223.7	259.6	258.4	172.2	3 250	
	13	50	171 000	210.0	32	.344	.259	.46	211.6	254.6	254.2	161.9	4 000	
	14	100	170 500	210.1	↓	.359	.313	1.02	213.6	255.9	255.7	163.4	4 040	
	15	200	171 000	210.0	↓	.375	.334	2.18	217.3	259.0	258.5	167.8	4 130	
	16	400	170 000	210.2	↓	.375	.344	4.43	224.2	265.7	263.9	172.3	4 190	
	17	50	229 000	210.3	42	.375	.250	.45	211.8	257.7	257.3	163.1	5 010	
	18	100	231 000	↓	↓	.375	.297	.97	213.6	262.4	261.8	164.9	4 760	
	19	200	234 000	↓	↓	.375	.325	2.13	217.4	266.7	265.6	168.7	4 800	
	20	400	233 000	↓	↓	.391	.344	4.43	224.3	271.7	270.6	173.1	4 970	
	21	50	350 000	210.3	62	.375	.250	.45	211.8	266.6	265.6	163.4	6 450	
	22	100	346 000	210.3	↓	.406	.297	.97	213.6	267.7	267.2	166.4	6 430	
	23	200	350 000	210.4	↓	.375	.313	2.06	217.3	273.6	272.2	169.4	6 300	
	24	400	347 000	210.3	↓	.406	.341	4.40	224.2	281.5	281.3	174.0	6 060	
	25	50	467 000	210.0	81	.406	.250	.45	211.5	273.3	272.6	164.8	7 600	
	26	100	465 000	210.0	↓	---	.281	.92	213.2	274.1	273.6	166.8	7 660	
	27	200	466 000	210.0	↓	---	.313	2.06	216.9	279.9	278.8	169.4	7 460	
	28	400	463 000	209.8	↓	---	.344	4.43	223.8	287.2	286.3	173.2	7 360	
	29	100	687 000	210.3	119	----	.281	.92	213.5	283.2	282.6	164.8	9 900	
	30	200	687 000	210.4	119	----	.297	1.96	217.0	286.1	285.0	169.2	10 010	
	31	400	690 000	210.3	119	----	.328	4.26	223.8	292.7	292.3	169.5	10 030	
	32	400	818 000	----	---	----	328	----	----	----	----	----	-----	Stable boiling; electrical failure

TABLE III. - Continued. EXPERIMENTAL DATA

(b) SI Units

Run	Data point	Rotative acceleration, a g	Heat flux, \dot{Q} A, m^2 KW	Vapor exit saturation temperature, $T_{\text{sat}, V}$ K	Liquid flow rate, kg/hr	Two-phase fluid annulus thickness, $h_{2\phi}^*$ cm	Non-boiling liquid annulus thickness, h^* cm	Pressure rise across fluid annulus, Δp , KN m^2	Wall surface saturation temperature, $T_{\text{sat}, W}$ K	Wall surface temperature, T_W K	Local two-phase fluid temperature, $T_{2\phi}$ K	Liquid inlet temperature, $T_{\text{in}, l}$ K	Boiling heat-transfer coefficient, $A(T_w - T_{\text{sat}, w})$ $\text{KW (m}^2\text{)(K)}$	Remarks
1	2	15	32.02	372.4	----	0.478	0.160	0.414	372.5	381.1	371.5	349.4	3.71	
	3	25	32.02	↓	----	.635	.478	1.38	372.8	381.3	371.1	349.7	3.76	
	4	50	31.55	↓	----	.795	.635	3.10	373.3	381.8	370.0	350.1	3.69	
	5	100	30.86	↓	----	.874	.795	7.03	374.3	381.9	369.9	351.2	4.07	
	7	200	29.91	↓	----	.889	.833	14.5	376.3	382.8	368.6	353.4	4.55	
	8	400	28.71	372.2	----	1.113	1.031	35.8	381.2	385.4	366.4	357.8	6.78	
	9	15	106.0	372.4	----	.874	.556	1.03	372.7	383.9	371.5	349.4	9.45	
	10	25	106.0	↓	----	1.112	.874	2.07	372.9	384.3	371.5	350.8	9.34	
	11	50	105.4	↓	----	1.191	1.031	4.48	373.7	385.2	371.2	352.1	9.17	
	12	100	104.7	↓	----	1.311	1.191	10.1	375.2	386.0	370.6	352.9	9.65	
	13	200	103.8	↓	----	1.191	1.112	19.0	377.4	387.4	369.7	355.0	10.4	
	14	400	102.5	↓	----	1.031	.953	33.1	380.7	389.7	366.4	359.9	11.5	
	15	15	179.8	372.4	4.8	1.031	.635	1.10	372.7	386.1	371.5	349.2	13.5	
	16	25	179.8	↓	↓	1.031	.556?	1.52	372.8	386.8	371.5	350.2	12.9	
	17	50	179.2	↓	↓	1.349	1.112	4.83	373.8	387.7	371.5	351.2	12.9	
	18	100	178.9	↓	↓	1.349	1.191	10.1	375.2	388.6	370.8	353.3	13.3	
	19	200	177.9	372.3	↓	1.285	1.230	20.7	377.7	390.4	369.6	354.7	14.0	
	20	400	176.7	372.3	↓	1.191	1.151	39.3	382.1	393.6	368.5	358.2	15.4	
	21	15	364.7	372.3	9.5	1.230	.714	1.24	372.7	388.2	371.7	348.6	23.6	
	22	25	364.7	↓	↓	1.112	.874	2.14	372.9	388.7	371.7	349.2	23.0	
	23	50	364.4	↓	↓	1.27	1.113	4.83	373.8	390.1	371.1	349.6	22.4	
	24	100	363.8	↓	↓	1.43	1.27	10.7	375.2	390.7	371.1	352.4	23.6	
	25	200	363.1	↓	↓	1.349	1.27	21.4	377.9	393.1	369.8	354.8	23.9	
	26	400	361.9	↓	↓	1.112	1.031	35.8	381.3	395.9	369.2	358.7	24.9	
	27	15	555.3	372.3	14.1	1.51	1.11	1.59	372.8	389.9	371.8	349.3	32.5	
	28	25	↓	↓	↓	1.51	1.27	2.83	373.1	390.4	371.8	349.7	32.0	
	29	50	↓	↓	↓	1.59	1.43	5.93	374.0	391.5	371.1	351.2	31.7	
	30	100	↓	↓	↓	1.67	1.51	12.4	375.7	392.6	370.7	353.8	32.7	
	31	200	↓	↓	↓	1.59	1.51	24.8	378.7	395.2	370.4	356.5	33.7	
	32	400	↓	↓	↓	1.35	1.27	42.7	382.8	399.3	369.3	361.4	33.7	
2	1	25	32.02	372.4	----	.635	.478	1.38	372.8	383.3	371.3	338.8	3.04	
	2	25	32.02	372.4	----	.635	.478	1.38	372.8	383.0	371.3	350.3	3.13	
	3	25	32.02	372.4	----	.635	.478	1.38	372.8	382.8	-----	356.4	3.18	
	4	25	106.0	372.4	----	.714	.460	1.38	372.8	385.9	-----	335.2	8.09	
	5	↓	↓	372.4	----	↓	.460	↓	372.8	385.9	-----	341.7	8.09	
	6	↓	↓	372.4	----	↓	.478	↓	372.8	386.1	-----	348.8	7.98	
	7	↓	↓	372.3	----	↓	.460	↓	372.7	386.2	-----	353.2	7.89	
	8	25	217.1	372.3	5.9	.714	.414	1.31	372.6	387.7	-----	335.1	14.4	
	9	↓	↓	↓	↓	↓	.437	↓	372.7	387.7	-----	341.9	14.4	
	10	↓	↓	↓	↓	↓	.437	↓	372.6	387.8	-----	349.5	14.2	
	11	↓	↓	↓	↓	↓	.437	↓	372.6	387.9	-----	355.6	14.1	

TABLE III. - Continued. EXPERIMENTAL DATA

(b) Continued. SI Units

Run	Data point	Rotative acceleration, a/g	Heat flux, Q/A , W/m^2	Vapor exit saturation temperature, $T_{\text{sat}, V}$, K	Liquid flow rate, kg/hr	Two-phase fluid annulus thickness, $h_{2\phi}'$, cm.	Non-boiling liquid annulus thickness, h_1' , cm.	Pressure rise across fluid annulus, Δp , kN/m^2	Wall surface saturation temperature, $T_{\text{sat}, W}$, K	Wall surface temperature, T_W , K	Local two-phase fluid temperature, $T_{2\phi}'$, K	Liquid inlet temperature, $T_{\text{in}, l}$, K	Boiling heat-transfer coefficient, $\frac{Q}{A(T_W - T_{\text{sat}, W})}$, average, $\frac{\text{W}}{(\text{m}^2)(\text{K})}$	Remarks
3	1	200	29.97	372.4	----	0.874	0.841	14.9	376.3	381.9	369.9	347.1	5.39	
	2	↓	↓	↓	----	.874	.841	↓	↓	382.0	369.9	352.5	5.29	
	3	↓	↓	↓	----	.874	.848	↓	↓	382.1	370.1	354.4	5.19	
	4	↓	↓	↓	----	-----	-----	↓	↓	382.2	369.8	358.9	5.09	
	5	200	103.8	372.4	----	.874	.833	14.8	376.3	387.3	370.6	346.3	9.39	
	6	↓	↓	372.4	----	↓	↓	↓	376.3	387.4	370.5	348.4	9.31	
	7	↓	↓	372.4	----	↓	↓	↓	376.3	387.6	370.4	350.1	9.22	
	8	↓	↓	372.3	----	↓	↓	↓	376.2	387.2	370.4	355.1	9.48	
	9	200	216.7	372.4	5.4	.912	.833	14.8	376.3	391.3	370.9	343.6	14.5	
	10	↓	↓	372.4	↓	↓	↓	↓	376.3	391.2	370.9	347.8	14.6	
	11	↓	↓	372.3	↓	↓	↓	↓	376.2	391.2	370.9	352.0	14.5	
	12	↓	↓	372.3	↓	↓	↓	↓	376.2	391.1	371.1	356.7	14.6	
	13	200	363.5	372.3	9.5	.912	.810	14.5	376.2	394.1	370.5	347.0	20.3	
	14	200	363.5	372.3	9.5	.912	.810	14.5	376.2	394.2	371.3	350.0	20.3	
	15	200	363.5	372.3	9.5	.912	.810	14.5	376.2	394.2	371.0	360.3	20.3	
4	1	25	32.18	372.4	----	1.11	.874	2.07	373.0	382.7	371.0	339.0	3.31	
	2	↓	106.0	↓	----	.714	.396	1.17	372.8	387.5	371.1	345.9	7.18	
	3	↓	180.5	↓	4.5	.795	↓	↓	↓	388.6	371.3	346.9	11.4	
	4	↓	366.0	↓	10.0	↓	↓	↓	↓	390.3	371.7	346.2	21.0	
	5	↓	555.3	↓	15.0	↓	↓	↓	↓	392.3	371.9	347.1	28.4	
	6	↓	735.1	372.5	19.5	↓	↓	↓	↓	394.1	372.1	349.4	34.5	
	7	↓	1120	372.5	29.1	↓	↓	↓	↓	397.3	372.4	351.1	45.7	
	8	↓	549.0	372.5	15.0	.714	↓	↓	↓	393.6	372.1	352.3	26.4	
	9	↓	372.3	372.4	10.4	↓	↓	↓	↓	390.3	372.0	352.4	21.2	
	10	↓	189.3	372.5	5.0	↓	.437	1.24	↓	387.8	371.7	352.8	12.6	
	11	↓	107.3	372.5	----	↓	.452	1.24	↓	386.6	371.3	353.2	7.77	
	12	↓	32.18	372.5	----	↓	.493	1.38	↓	383.4	370.6	353.8	3.05	
5	13	25	32.18	372.5	----	0.676	0.437	1.24	372.8	382.9	370.6	356.9	3.20	
	14	↓	107.3	↓	----	.714	.422	1.24	↓	386.9	371.3	355.3	7.60	
	15	↓	220.9	↓	5.9	.714	.414	1.17	↓	389.2	371.6	353.4	13.5	
	16	↓	444.9	↓	11.8	.714	.396	1.17	↓	391.9	371.8	351.4	23.3	
	17	↓	662.6	372.4	17.7	.754	.396	1.17	↓	394.3	371.9	351.3	30.7	
	18	↓	946.5	↓	25.0	.795	.381	1.10	↓	396.8	372.1	352.2	39.4	
	19	↓	567.9	↓	15.0	.795	.396	1.17	↓	392.9	371.8	353.2	28.1	
	20	↓	295.0	↓	8.2	.754	.396	1.17	↓	389.9	371.7	353.6	17.2	
	21	↓	106.0	↓	----	.795	.478	1.38	↓	386.9	371.0	354.4	7.49	

TABLE III. - Continued. EXPERIMENTAL DATA

(b) Continued. SI Units

Run	Data point	Rota- tive acceler- ation, a g	Heat flux, Q A, kW m ²	Vapor exit satura- tion tempera- ture, T _{sat, v} , K	Liquid flow rate, kg hr	Two- phase fluid annulus thickness, h _{2o} , cm.	Non- boiling liquid annulus thickness, h', cm.	Pressure rise across fluid annulus, Δp, kN m ⁻²	Wall surface satura- tion tempera- ture, T _{sat, w} , K	Wall surface tempera- ture, T _w , K		Local two- phase fluid tempera- ture, T _{2o} , K	Liquid inlet tempera- ture, T _{in} , K	Boiling heat- transfer coefficient, Q average, kW (m ²)(K)	Remarks
										High	Low				
6	1	200	29.56	372.4	----	0.795	0.754	13.4	376.1	382.9	382.3	369.1	354.2	4.51	Boiling interrupted prior to point
	2		104.1	372.4	----	.795	.754	13.4	376.1	388.7	388.3	370.0	353.3	8.34	
	3		181.7	372.5	5.0	.833	.754	13.4	376.1	391.8	390.8	370.4	357.8	11.9	
	4		366.0	372.4	10.0	.833	.739	13.1	375.9	395.8	395.4	370.9	357.1	18.6	
	5		555.3	372.4	15.0	.874	.732	13.1	375.9	398.1	397.8	370.9	357.1	25.2	
	6		747.7	372.4	20.0	.912	.721	13.1	375.9	399.8	399.7	371.3	358.7	31.4	
	7		1104	372.5	29.1	----	.691	12.4	375.8	402.7	402.5	371.4	360.3	41.2	
	8		1492	372.5	37.7	----	.556	10.3	375.2	404.9	404.8	371.1	361.3	50.3	
	9		747.7	372.4	20.4	.874	.714	12.8	375.8	400.6	400.2	370.3	361.7	30.2	
	10		366.0	372.4	10.0	.874	.732	13.1	375.9	398.0	397.6	370.8	361.3	16.7	
	11		181.7	372.3	5.0	.833	.747	13.4	375.9	392.4	391.9	369.5	360.9	11.2	
	12		103.8	372.3	----	----	----	13.4	375.9	388.5	388.2	----	358.6	8.34	
	13		26.19	372.5	----	.795	.754	13.4	376.1	382.0	381.8	369.5	359.2	4.51	
	14		364.4	372.4	9.5	.874	.739	13.1	375.9	397.7	397.3	370.7	354.7	16.9	
	15		366.0	372.4	9.5	.874	.732	13.1	375.9	397.7	397.1	371.0	350.6	17.1	
7	1	200	104.1	372.6	----	----	1.59	25.6	379.1	391.2	390.4	369.1	353.3	8.82	Boiling interrupted prior to point
	2		179.8	362.6	5.0	----	1.35	22.4	379.3	393.1	391.9	369.4	357.0	12.7	
	3		370.1	372.5	11.4	----	1.27	21.4	378.1	398.0	397.7	370.3	356.0	18.7	
	4		552.1	372.6	16.0	1.19	1.11	19.0	377.5	399.9	399.5	370.2	354.2	24.8	
	5		750.9	372.6	20.0	1.15	1.03	17.9	377.2	401.2	400.8	370.7	355.2	31.5	
	6		1107	372.6	29.1	----	.912	15.9	376.7	403.2	402.9	371.0	356.7	42.0	
	7		741.4	372.6	20.0	1.19	1.11	19.0	377.5	401.7	401.3	370.2	358.1	30.9	
	8		367.6	372.6	9.5	----	1.39	22.8	378.4	399.1	398.5	370.2	362.3	18.0	
	9		178.3	372.6	4.5	----	1.83	28.6	379.8	394.4	391.7	368.9	360.1	13.4	

TABLE III. - Continued. EXPERIMENTAL DATA

(b) Continued. SI Units

Run	Data point	Rotative acceleration, a/g	Heat flux, Q/A , kW m ⁻²	Vapor exit saturation temperature, $T_{\text{sat}, V}$, K	Liquid flow rate, kg/hr	Two-phase fluid annulus thickness, $h_{2,0}'$, cm.	Non-boiling liquid annulus thickness, h' , cm.	Pressure rise across fluid annulus, Δp , kN, m ²	Wall surface saturation temperature, $T_{\text{sat}, W}$, K	Wall surface temperature, T_W , K		Local two-phase fluid temperature, $T_{2,0}$, K		Liquid inlet temperature, T_{in} , K	Boiling heat-transfer coefficient, $\frac{Q}{A(T_W - T_{\text{sat}, W})}$ average, $\frac{\text{kW}}{\text{m}^2(\text{K})}$	Remarks
										High	Low	High	Low			
8	1	200	104.1	372.4	0	---	1.27	21.4	378.0	389.1	388.2	369.1	367.9	----	9.82	Feed system valved off
	2	200	104.1	372.4	0	---	.953	16.6	376.8	388.8	388.2	369.7	368.7	----	8.91	
	3	200	104.1	372.4	0	---	.635	11.5	376.6	388.0	387.8	369.4	368.8	----	8.43	
	4	200	178.9	372.4	0	---	1.59	25.6	378.9	394.0	392.7	369.7	368.6	----	12.4	Feed system valved off
	5	↓	↓	↓	↓	---	1.27	21.4	378.0	393.8	392.7	369.8	368.5	----	11.7	
	6	↓	↓	↓	↓	---	.953	16.6	376.8	393.3	392.6	369.8	369.0	----	11.1	
	7	↓	↓	↓	↓	---	.635	11.5	376.6	392.7	392.3	370.3	369.8	----	10.6	↓
	8	↓	↓	↓	↓	---	.556	10.2	376.2	393.2	392.8	370.7	370.2	----	10.0	
	9	↓	↓	↓	↓	---	---	---	---	---	---	---	---	----	---	
	10	200	271.3	372.4	0	---	1.27	21.4	378.0	396.8	396.3	369.9	----	----	14.6	Feed system valved off (unre- liable liquid level)
	11	↓	↓	↓	↓	---	.953	16.6	376.8	396.2	396.1	----	----	14.0		
	12	↓	↓	↓	↓	---	.635	11.5	375.6	395.7	395.3	370.7	----	13.6		
	13	↓	↓	↓	↓	---	.478	8.96	374.9	395.2	394.9	370.7	----	13.4	↓	
	14	200	364.4	372.4	0	---	1.27	21.4	378.0	398.6	398.3	----	----	17.8		
	15	↓	↓	↓	↓	---	.953	16.6	376.8	397.9	397.6	----	----	17.4		
	16	↓	↓	↓	↓	---	.635	11.5	375.6	396.9	396.7	----	----	17.1	↓	
	17	↓	↓	↓	↓	---	.478	8.96	374.9	396.2	396.0	----	----	17.2		
9	1	25	32.02	372.6	0	---	1.27	2.90	373.3	383.1	382.7	371.4	370.8	----	3.35	Feed system valved off
	2	↓	↓	372.6	↓	---	.953	2.34	373.2	383.2	383.0	371.2	370.7	----	3.25	
	3	↓	↓	372.6	↓	---	.635	1.72	373.0	383.2	383.1	370.9	370.8	----	3.15	
	4	↓	↓	372.5	↓	---	.318	1.03	372.8	383.7	383.6	370.5	370.1	----	2.95	↓
	5	↓	↓	----	↓	---	.160	.69	372.7	384.7	384.4	371.2	370.3	----	2.71	
	6	25	106.0	372.5	0	---	1.27	2.90	373.3	387.2	386.8	371.8	371.2	----	7.69	
	7	↓	↓	372.5	↓	---	.953	2.34	373.2	387.1	386.7	371.4	371.3	----	7.69	Feed system valved off
	8	↓	↓	----	↓	---	.635	1.72	372.9	387.2	386.8	371.3	371.1	----	7.52	
	9	↓	↓	----	↓	---	.318	1.03	372.8	387.5	387.2	371.3	371.1	----	7.26	
	10	↓	↓	372.6	↓	---	.160	.69	372.7	387.7	387.6	372.4	372.3	----	7.09	↓
	11	25	106.0	372.4	0	---	.953	2.34	373.1	387.1	386.8	371.4	371.2	----	7.66	
	12	↓	↓	↓	↓	---	.635	1.72	372.9	387.2	386.9	----	----	7.46		
	13	↓	↓	↓	↓	---	.318	1.03	372.7	387.3	387.1	371.1	370.9	----	7.29	↓
	14	↓	↓	↓	↓	---	.160	.69	372.6	387.6	387.4	372.4	372.3	----	7.07	
	15	25	179.8	372.5	0	---	1.27	2.90	373.3	389.2	389.0	371.7	371.0	----	11.4	
	16	↓	↓	372.4	↓	---	.953	2.34	373.1	389.3	388.6	----	----	11.4	Feed system valved off	
	17	↓	↓	372.4	↓	---	.635	1.72	372.9	389.0	388.8	371.3	371.1	----		11.2
	18	↓	↓	----	↓	---	.318	1.03	372.7	389.1	389.0	----	----	11.0		
	19	↓	↓	----	↓	---	.160	.69	372.6	388.9	388.8	----	----	11.1	↓	
	20	25	272.0	372.4	0	---	1.27	2.90	373.2	391.1	390.4	371.4	371.2	----		15.5
	21	↓	↓	↓	↓	---	.953	2.34	373.1	390.7	390.6	----	----	15.5	Feed system valved off	
	22	↓	↓	↓	↓	---	.635	1.72	372.9	390.9	390.8	----	----	15.2		
	23	↓	↓	↓	↓	---	.318	1.03	372.7	390.6	390.5	----	----	15.3		
	24	↓	↓	↓	↓	---	.160	.69	372.6	390.6	390.5	----	----	15.2	↓	
	25	25	369.1	372.4	0	---	1.27	2.90	373.2	392.5	392.4	----	----	19.2		
	26	↓	↓	↓	↓	---	.953	2.34	373.1	392.4	392.3	----	----	19.2	Feed system valved off	
	27	↓	↓	↓	↓	---	.635	1.72	372.9	392.2	392.2	----	----	19.1		
	28	↓	↓	↓	↓	---	.318	1.03	372.7	392.1	392.0	----	----	19.1		
	29	↓	↓	↓	↓	---	.160	.69	372.6	391.9	391.9	----	----	19.1	↓	

TABLE III. - Continued. EXPERIMENTAL DATA

(b) Continued. SI Units

Run	Data point	Rota- tive acceler- ation, a, g	Heat flux, Q, A, m^2 kW/m ²	Vapor exit satura- tion tempera- ture, T _{sat, v} , K	Liquid flow rate, kg/hr	Two- phase fluid annulus thickness, h _{2φ} , cm.	Non- boiling liquid annulus thickness, h', cm.	Pressure rise across fluid annulus, Δp, kN/m ²	Wall surface satura- tion tempera- ture, T _{sat, w} , K	Wall surface tempera- ture, T _w , K		Local two- phase fluid tempera- ture, T _{2φ} , K		Liquid inlet tempera- ture, T _{in, l} , K	Boiling heat- transfer coefficient, Q A(T _w - T _{sat, w}) average, kW (m ²)(K)	Remarks
										High	Low	High	Low			
10	1	25	32.02	372.4	0	----	1.27	2.90	373.2	382.4	382.2	370.8	370.4	----	3.52	Feed system valved off ↓
	2	↓	↓	372.3	↓	----	.953	2.34	373.0	382.9	382.5	371.0	370.7	----	3.30	
	3	↓	↓	↓	↓	----	.635	1.72	372.7	382.7	382.6	370.9	370.8	----	3.24	
	4	↓	↓	↓	↓	----	.318	1.03	372.6	383.3	383.2	370.9	370.7	----	3.02	
	5	↓	↓	↓	↓	----	.160	.69	372.5	383.8	383.7	372.3	----	2.84		
	6	25	106.0	372.4	0	----	1.27	2.90	373.2	386.6	386.2	371.7	371.1	----	7.97	Feed system valved off ↓
	7	↓	↓	↓	↓	----	.953	2.34	373.1	386.2	386.0	371.1	370.7	----	8.12	
	8	↓	↓	↓	↓	----	.635	1.72	372.8	386.9	386.7	371.3	370.8	----	7.55	
	9	↓	↓	↓	↓	----	.318	1.03	372.7	387.2	387.1	----	----	7.32		
	10	↓	↓	↓	↓	----	.160	.69	372.6	387.3	387.2	371.6	371.4	----	7.21	
	11	25	179.8	372.4	0	----	1.27	2.90	373.2	389.1	388.6	371.6	371.4	----	11.5	Feed system valved off ↓
	12	↓	↓	372.4	↓	----	.953	2.34	373.1	388.6	388.0	371.4	370.9	----	11.8	
	13	↓	↓	372.3	↓	----	.635	1.72	372.8	388.7	388.5	371.4	371.3	----	11.4	
	14	↓	↓	372.3	↓	----	.318	1.03	372.6	388.7	388.6	----	----	11.2		
	15	↓	↓	372.3	↓	----	.160	.69	372.5	389.2	389.1	----	----	10.8		
	16	25	282.1	372.3	0	----	1.27	2.90	373.1	390.5	390.2	----	----	----	16.3	Feed system valved off ↓
	17	↓	↓	↓	↓	----	.953	2.34	372.9	390.3	390.2	----	----	----	16.3	
	18	↓	↓	↓	↓	----	.635	1.72	372.7	390.2	390.0	----	----	----	16.2	
	19	↓	↓	↓	↓	----	.318	1.03	372.6	390.1	390.1	----	----	----	16.1	
	20	↓	↓	↓	↓	----	.160	.69	372.4	390.1	390.1	----	----	----	16.0	
	21	25	366.0	372.3	0	----	1.27	2.90	373.1	391.1	391.0	----	----	----	20.4	Feed system valved off ↓
	22	↓	↓	↓	↓	----	.953	2.34	373.0	391.0	390.9	----	----	----	20.4	
	23	↓	↓	↓	↓	----	.635	1.72	372.8	391.1	391.0	----	----	----	20.0	
	24	↓	↓	↓	↓	----	.318	1.03	372.6	391.0	390.9	----	----	----	19.9	
	25	↓	↓	↓	↓	----	.160	.69	372.5	391.3	391.2	----	----	----	19.5	
	26	25	179.8	372.4	---	----	.437	1.31	372.7	388.9	388.8	371.3	371.2	----	11.1	Feed resumed

TABLE III. - Continued. EXPERIMENTAL DATA

(b) Continued. SI Units

Run	Data point	Rotative acceleration, a g	Heat flux, Q A, kW m ²	Vapor exit saturation temperature, T _{sat, V} K	Liquid flow rate, kg hr	Two-phase fluid annulus thickness, h _{2, C} , cm.	Non-boiling liquid annulus thickness, h', cm.	Pressure rise across fluid annulus, Δp, kN m ²	Wall surface saturation temperature, T _{sat, W} K	Wall surface temperature, T _w , K		Local two-phase fluid temperature, T _{2, C} , K		Liquid inlet temperature, T _{in, l} , K	Boiling heat-transfer coefficient, $\frac{Q}{A(T_w - T_{sat, w})}$ average, kW (m ²)(K)	Remarks
										High	Low	High	Low			
11	1	25	4.32	372.0	-----	-----	0.833	2.07	372.6	376.8	376.8	371.1	370.9	342.8	1.03	Boiling
	2	↓	13.57	371.9	-----	-----	.833	2.07	372.6	379.2	379.1	370.6	370.4	346.2	2.06	↓
	3	↓	32.02	372.0	-----	0.833	.714	1.86	372.6	382.6	382.4	370.2	370.1	348.2	3.22	↓
	4	↓	4.32	371.9	-----	.754	.714	1.86	372.4	376.9	376.9	371.1	370.9	349.4	.97	↓
	5	50	3.69	372.1	-----	-----	.833	3.79	373.1	378.1	378.1	370.7	370.4	351.3	.74	Boiling
	6	↓	12.93	372.0	-----	.795	.754	3.52	373.0	379.3	379.3	370.2	369.9	351.7	2.05	↓
	7	↓	31.55	371.8	-----	.754	.714	3.38	372.8	382.4	382.2	370.3	370.1	352.7	3.31	↓
	8	↓	3.69	371.9	-----	-----	.754	3.52	372.9	376.8	376.7	370.8	370.6	352.4	.97	↓
	9	100	3.08	371.9	-----	-----	.874	7.72	374.1	378.3	378.2	370.0	369.8	353.1	.74	Boiling
	10	↓	12.34	372.0	-----	-----	.833	7.38	374.1	379.9	379.7	369.7	369.5	354.0	2.14	↓
	11	↓	30.82	372.1	-----	.874	.795	7.03	374.0	382.7	382.6	370.0	369.6	354.3	3.56	↓
	12	↓	3.08	372.1	-----	-----	.874	7.72	374.3	378.1	378.1	370.0	369.6	352.6	.81	↓
	13	200	2.16	372.0	-----	-----	.953	16.6	376.4	377.7	377.7	369.3	369.1	351.3	----	Natural convection
	14	↓	11.39	372.1	-----	-----	.874	15.5	376.2	381.0	380.7	368.2	367.8	352.1	2.47	Boiling
	15	↓	20.67	372.1	-----	-----	.859	15.2	376.1	381.2	381.1	368.6	368.2	353.8	4.11	Boiling
	16	↓	29.88	372.0	-----	-----	.848	15.1	376.1	383.4	383.4	369.0	368.9	355.4	4.07	Boiling
	17	↓	2.16	371.9	-----	-----	.912	16.0	376.2	377.2	377.1	369.5	369.4	352.2	----	Natural convection
	18	400	.92	372.0	-----	-----	.986	34.1	380.6	376.0	375.9	370.1	370.0	350.7	----	Natural convection
	19	↓	10.10	371.9	-----	-----	.953	33.1	380.3	380.0	379.9	367.8	367.4	350.8	----	Natural convection
	20	↓	19.43	↓	-----	-----	.953	33.1	380.3	383.3	383.2	365.9	365.6	351.7	----	Natural convection
	21	↓	28.71	↓	-----	-----	.912	31.9	380.1	384.9	384.8	365.6	365.1	352.6	5.61	Boiling
	22	↓	47.33	↓	-----	-----	.912	31.9	380.1	387.6	387.3	366.3	364.7	353.1	6.38	Boiling
12	1	400	.92	371.9	-----	-----	0.953	33.1	380.3	374.4	374.3	370.7	370.4	344.4	----	Natural convection
	2	↓	10.10	371.8	-----	-----	.922	32.1	380.0	377.5	377.4	368.2	367.9	346.3	----	Natural convection
	3	↓	19.43	371.9	-----	-----	.912	31.9	380.1	382.2	382.2	366.4	366.2	347.6	----	Natural convection
	4	↓	28.71	371.9	-----	-----	.912	31.9	380.0	385.1	384.6	366.6	365.8	349.3	5.96	Boiling
	5	↓	47.33	371.8	-----	-----	.912	31.9	379.9	386.6	386.4	367.7	366.6	350.1	7.18	Boiling
	6	↓	.92	371.8	-----	-----	.930	32.3	380.0	374.9	374.8	370.3	370.0	348.4	----	Natural convection
	7	200	2.15	371.8	-----	-----	1.016	17.6	376.5	376.4	376.3	369.4	369.2	348.8	----	Natural convection
	8	↓	11.42	↓	-----	-----	.953	16.6	376.2	380.5	380.4	369.4	368.7	349.4	2.71	Boiling
	9	↓	20.67	↓	-----	-----	.889	15.7	376.0	381.3	381.2	369.3	369.1	351.1	3.92	Boiling
	10	↓	29.88	↓	-----	-----	.848	15.1	375.8	382.2	382.1	369.2	368.3	352.7	4.76	Boiling
	11	100	3.08	371.8	-----	-----	.953	8.41	374.2	377.2	377.2	370.1	369.8	350.8	1.02	Boiling
	12	100	12.30	371.8	-----	-----	.866	7.65	373.9	379.2	378.7	369.6	369.3	352.1	2.46	Boiling
	13	100	30.79	371.8	-----	-----	.833	7.38	373.9	381.8	381.7	369.1	368.7	353.3	3.90	Boiling
	14	50	3.70	371.8	-----	-----	.795	3.65	372.8	377.3	377.2	370.2	369.8	353.3	.84	Boiling
	15	50	12.94	371.8	-----	-----	.754	3.52	372.8	380.2	380.1	369.7	369.5	354.1	1.77	Boiling
	16	50	31.42	371.8	-----	-----	.714	3.38	372.8	382.7	382.6	369.9	369.7	354.1	3.18	Boiling
	17	25	4.32	371.8	-----	-----	.635	1.72	372.3	377.4	377.4	370.8	370.7	355.2	.85	Boiling
	18	25	13.57	371.8	-----	-----	.572	1.59	372.3	379.5	379.4	370.2	369.6	356.4	1.88	Boiling
	19	25	32.02	371.8	-----	-----	.516	1.45	372.2	382.4	382.3	370.4	369.9	356.5	3.15	Boiling

TABLE III. - Continued. EXPERIMENTAL DATA

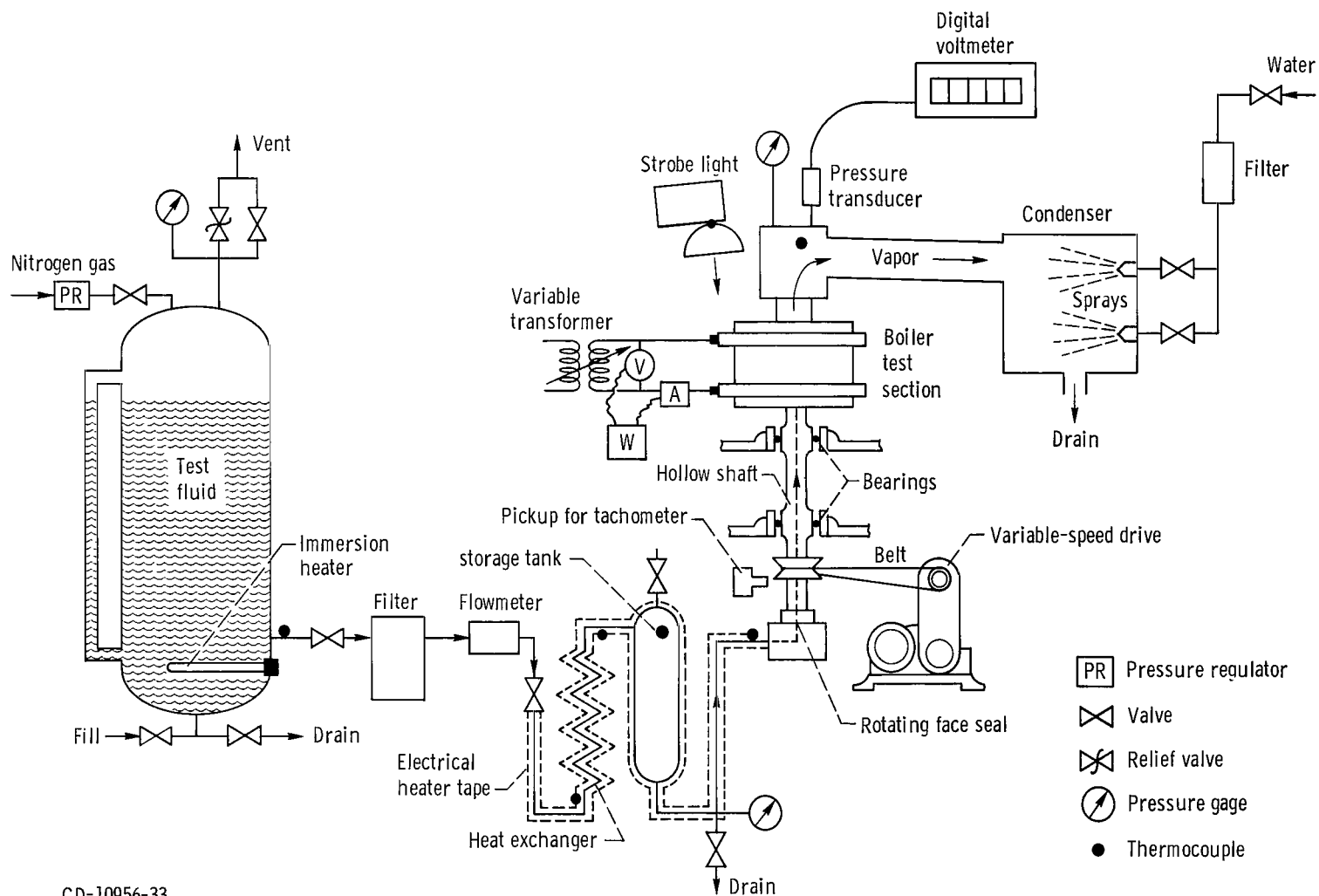
(b) Continued. SI Unit-

Run	Data point	Rotative acceleration, a g	Heat flux, Q/A , kW/m ²	Vapor exit saturation temperature, $T_{sat, V}$, K	Liquid flow rate, kg/hr	Two-phase fluid annulus thickness, $h_{2,0}$, cm	Non-boiling liquid annulus thickness, h' , cm	Pressure rise across fluid annulus, Δp , kN/m ²	Wall surface saturation temperature, $T_{sat, W}$, K	Wall surface temperature, T_w , K	Local two-phase fluid temperature, $T_{2,0}$, K		Distance from wall of local two-phase fluid TC, cm	Liquid inlet temperature, $T_{in, l}$, K	Boiling heat-transfer coefficient, $Q/(A(T_w - T_{sat, w}))$, kW/(m ²)(K)	Remarks
											High	Low				
13	1	25	87.71	372.2	---	---	0.795	2.07	372.7	384.8	370.1	369.7	0.079	340.6	7.25	
	2	↓	↓	↓	---	---	.833	↓	372.8	384.7	371.3	370.9	.238	345.2	7.38	
	3	↓	↓	↓	---	---	.795	↓	372.8	384.2	371.6	371.2	.397	350.4	7.66	
	4	↓	↓	↓	---	---	---	↓	372.7	384.5	372.1	372.0	.556	350.9	7.43	
	5	↓	↓	372.0	---	---	---	↓	372.6	384.4	372.6	372.2	.714	352.6	7.41	
	6	↓	↓	372.0	---	---	---	↓	372.6	384.2	371.9	371.8	.873	355.1	7.55	
	7	↓	↓	372.0	---	---	---	↓	372.6	384.4	372.1	372.0	1.03	354.4	7.38	
	8	↓	↓	371.9	---	---	---	↓	372.5	384.6	370.2	369.9	.159	356.3	7.26	
	9	25	366.0	371.9	---	---	.437	1.24	372.3	391.4	370.1	369.8	.079	353.3	19.1	
	10	↓	↓	372.0	---	---	---	↓	---	391.5	370.9	370.7	.238	354.2	19.1	
	11	↓	↓	372.0	---	---	---	↓	---	391.6	371.6	371.4	.397	355.5	19.0	
	12	↓	↓	372.0	---	---	---	↓	---	391.7	371.7	371.6	.556	354.2	18.9	
	13	↓	↓	371.9	---	---	---	↓	---	391.4	372.0	372.0	.714	354.3	19.1	
	14	↓	↓	371.9	---	---	---	↓	---	391.5	371.8	371.8	.794	355.2	19.0	
	15	200	85.50	371.9	---	---	.874	15.5	376.1	386.4	368.9	368.4	.079	355.4	8.31	
	16	↓	↓	371.9	---	---	.874	15.5	376.1	386.9	368.8	367.9	.238	355.6	7.89	
	17	↓	↓	371.8	---	---	.833	14.8	375.8	386.9	369.5	368.8	.397	356.0	7.75	
	18	↓	↓	371.9	---	---	---	↓	375.9	386.7	369.4	368.7	.556	356.3	7.89	
	19	↓	↓	371.8	---	---	---	↓	375.8	386.8	369.8	369.3	.714	355.7	7.77	
	20	↓	↓	371.9	---	---	---	↓	375.9	386.7	370.1	370.0	.873	356.3	7.89	
	21	↓	↓	371.9	---	---	---	↓	375.9	386.4	372.0	371.9	1.03	356.4	8.17	
	22	↓	↓	372.0	---	---	---	↓	376.0	386.2	371.7	371.1	.953	355.9	8.34	
	23	200	362.8	372.1	---	---	.833	14.8	376.1	395.5	370.0	368.3	.079	353.0	18.7	
	24	↓	↓	372.1	---	---	---	↓	376.1	395.6	369.9	368.1	.238	352.4	18.6	
	25	↓	↓	372.0	---	---	---	↓	376.0	395.3	370.7	369.6	.397	352.6	18.7	
	26	↓	↓	371.9	---	---	---	↓	375.9	395.8	370.5	369.7	.556	352.0	18.3	
	27	↓	↓	↓	---	---	---	↓	---	395.4	370.8	370.2	.714	353.1	18.6	
	28	↓	↓	↓	---	---	---	↓	---	395.8	371.3	370.6	.873	353.4	18.3	
	29	↓	↓	↓	---	---	---	↓	---	395.4	371.9	371.7	1.03	354.3	18.6	
14	1	400	84.55	371.8	0	---	0.953	33.1	380.2	388.5	366.8	366.5	.635	353.3	10.2	Feed system
	2	↓	↓	↓	↓	---	.874	30.6	379.6	---	367.2	366.7	---	355.5	---	valved off
	3	↓	↓	↓	↓	---	.795	28.1	379.1	---	368.1	367.6	---	---	---	
	4	↓	↓	↓	↓	---	.714	25.5	378.4	387.6	368.3	367.6	---	---	9.31	
	5	↓	↓	371.9	↓	---	.635	22.8	377.9	---	369.4	369.2	---	---	---	
	6	↓	↓	↓	↓	---	.556	20.1	377.3	---	371.8	371.7	---	---	---	
	7	↓	↓	↓	↓	---	.478	17.6	376.6	---	372.2	372.1	---	---	---	
	8	↓	↓	↓	↓	---	.396	14.9	376.0	---	372.2	372.1	---	---	---	
	9	↓	↓	↓	↓	---	.318	12.1	375.2	---	372.3	372.2	---	---	---	
	10	↓	↓	↓	↓	---	.239	9.31	374.6	387.1	372.2	372.1	---	---	6.75	
	11	↓	↓	↓	↓	---	.160	6.34	373.7	---	372.2	---	↓	---	---	
	16	400	362.8	372.0	0	---	.795	28.1	379.2	398.5	369.5	368.9	.635	348.6	18.3	Points 12 to 15
	17	↓	↓	↓	↓	---	.635	22.8	378.0	---	369.9	369.3	---	---	---	unreliable; re-
	18	↓	↓	↓	↓	---	.478	17.6	376.7	---	372.1	371.9	---	---	---	peated as 16 to
	19	↓	↓	↓	↓	---	.318	12.1	375.3	---	372.2	372.2	---	---	---	20; feed system
	20	↓	↓	↓	↓	---	.160	6.34	373.8	---	372.2	372.1	↓	---	---	valved off

TABLE III. - Concluded. EXPERIMENTAL DATA

(b) Concluded. SI Units

Run	Data point	Rotational acceleration, α , g	Heat flux, Q , W m^{-2}	Vapor exit saturation temperature, $T_{\text{sat, v}}$, K	Liquid flow rate, \dot{m} , kg hr	Two-phase fluid annulus thickness, $h_{2, \text{tp}}$, cm	Non-boiling liquid annulus thickness, h' , cm	Pressure rise across fluid annulus, Δp , kN m^{-2}	Wall surface saturation temperature, $T_{\text{sat, w}}$, K	Wall surface temperature, T_w , K		Local two-phase fluid temperature, $T_{2, \text{cp}}$, K	Liquid inlet temperature, $T_{\text{in, l}}$, K	Boiling heat-transfer coefficient, Q_c , $\frac{\text{W}}{\text{m}^2(\text{K})}$	Remarks
										High	Low				
15	1	50	105.4	372.2	----	0.874	0.714	3.38	373.2	389.7	389.5	370.9	341.3	6.44	
	2	100	104.7	372.2	----	1.031	.795	7.03	374.2	389.4	389.2	370.6	345.7	6.90	
	3	200	104.4	372.1	----	.953	.859	15.2	376.2	389.3	388.8	369.8	347.5	8.12	
	4	400	103.2	372.2	----	.953	.904	31.5	380.2	390.3	390.1	367.2	350.8	10.3	
	5	50	176.7	372.2	----	.874	.714	3.38	373.2	390.7	390.4	371.4	345.1	10.2	
	6	100	171.3	372.2	----	.912	.795	7.03	374.1	391.7	391.3	370.6	345.8	9.85	
	7	200	170.7	372.1	----	.912	.859	15.2	376.2	392.2	391.9	369.8	347.7	10.8	
	8	400	169.4	371.9	----	.953	.889	31.0	379.8	392.9	391.8	368.3	349.7	13.5	
	9	50	367.6	372.0	9.5	.874	.714	3.38	373.0	393.8	393.6	371.7	344.6	17.7	
	10	100	364.4	372.1	↓	.912	.803	7.03	374.1	394.7	394.6	371.4	346.2	17.7	
	11	200	362.8	371.9	↓	.912	.866	15.3	376.1	396.9	396.6	370.4	348.1	17.5	
	12	400	361.2	371.8	↓	.953	.874	30.5	379.6	399.6	398.9	369.2	351.0	18.4	
	13	50	539.5	372.0	14.5	.874	.658	3.17	372.9	396.8	396.6	371.7	345.3	22.7	
	14	100	537.9	372.1	↓	.912	.795	7.03	374.0	397.5	397.4	371.5	346.1	22.9	
	15	200	539.5	372.0	↓	.953	.848	15.0	376.1	399.2	398.9	370.6	348.6	23.4	
	16	400	536.4	372.1	↓	.953	.874	30.5	379.9	402.9	401.9	369.3	351.1	23.8	
	17	50	722.5	372.2	19.1	.953	.635	3.10	373.0	398.5	398.3	371.9	345.9	28.4	
	18	100	728.8	↓	↓	.953	.754	6.69	374.0	401.1	400.8	371.7	346.9	27.0	
	19	200	738.3	↓	↓	.953	.826	14.7	376.1	403.5	402.9	370.9	349.1	27.2	
	20	400	735.1	↓	↓	.993	.874	30.5	379.9	406.3	405.7	370.2	351.5	28.2	
	21	50	1104	372.2	28.1	.953	.635	3.10	373.0	403.4	402.9	372.0	346.1	36.6	
	22	100	1092	↓	↓	1.031	.754	6.69	374.0	404.1	403.8	371.6	347.8	36.5	
	23	200	1104	↓	↓	.953	.795	14.2	376.1	407.3	406.6	370.8	349.4	35.8	
	24	400	1095	↓	↓	1.031	.866	30.3	379.9	411.7	411.6	369.5	352.0	34.4	Secondary cells rotating faster than boiler
	25	50	1473	372.0	36.8	1.031	.635	3.10	372.8	407.2	406.8	371.8	346.9	43.1	
	26	100	1467	372.0	↓	↓	.714	6.34	373.8	407.6	407.3	371.4	348.0	43.5	
	27	200	1470	372.0	↓	↓	.795	14.2	375.8	410.8	410.2	370.7	349.4	42.3	
	28	400	1461	371.9	↓	↓	.874	30.5	379.7	414.9	414.4	369.3	351.6	41.8	
	29	100	2167	372.2	54.0	----	.714	6.34	373.9	412.7	412.3	371.7	346.9	56.2	
	30	200	2167	372.2	54.0	----	.754	13.5	375.9	414.3	413.7	371.4	349.3	56.8	
	31	400	2177	372.2	54.0	----	.833	29.4	379.7	417.9	417.7	370.2	349.5	56.9	
	32	400	2581	----	----	----	.833	----	----	----	----	----	----	----	Stable boiling; electrical failure



CD-10956-33

Figure 1. - Schematic diagram of test apparatus for rotating boiler.

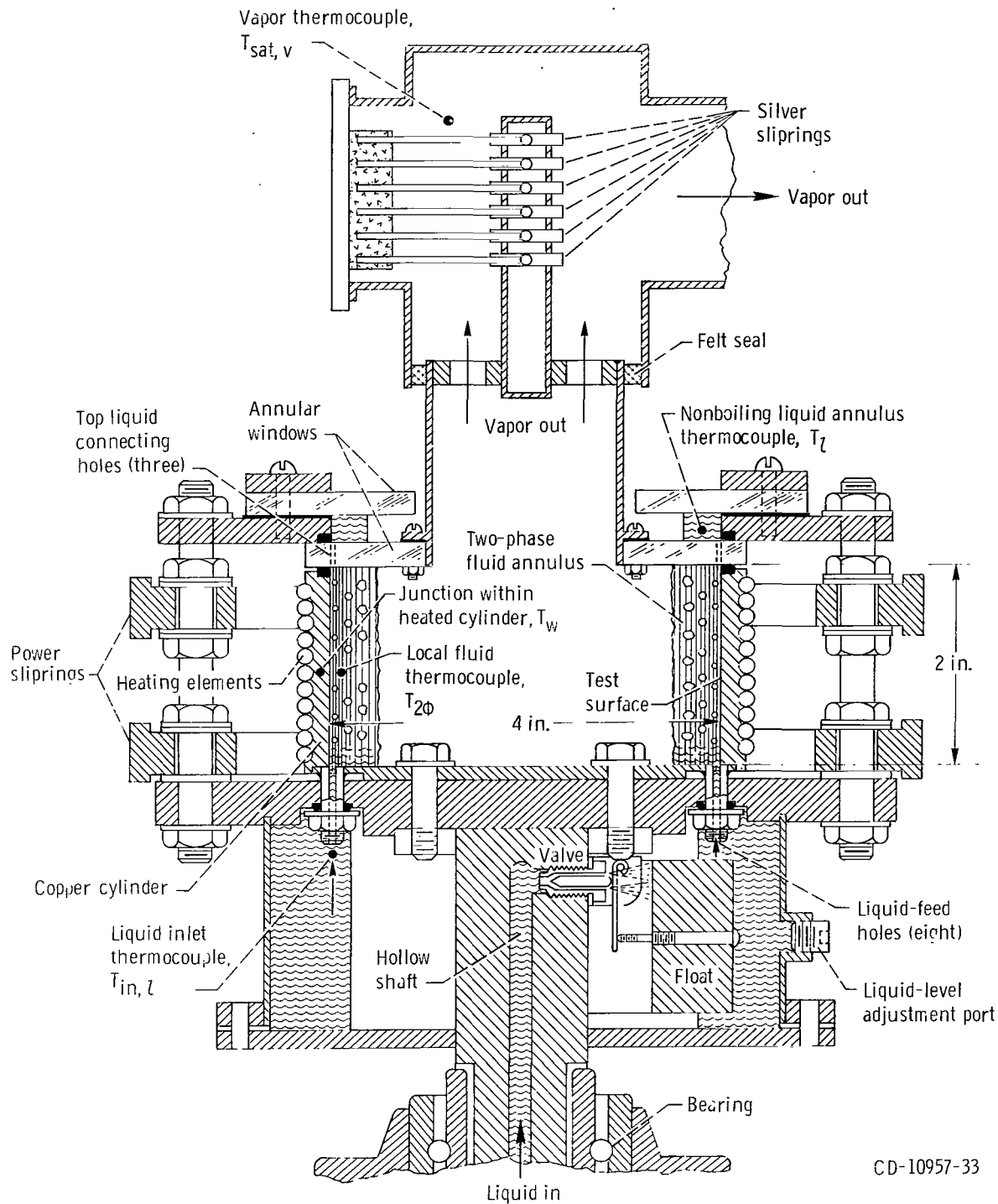


Figure 2. - Rotating boiler cross-section and thermocouple locations.

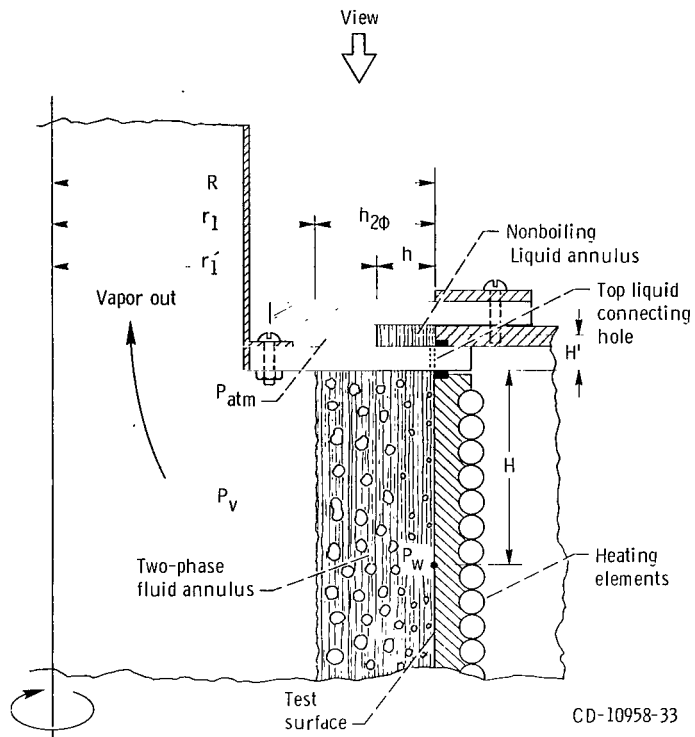


Figure 3. - Nomenclature for void fraction calculation.

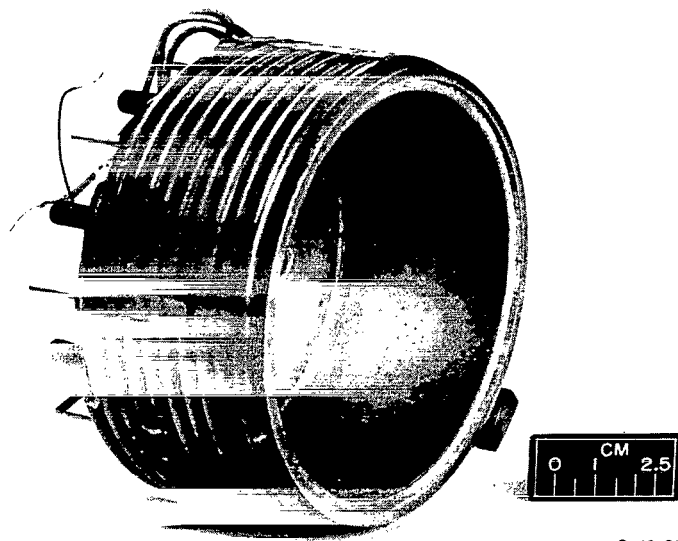


Figure 4. - View of test surface showing pitting.

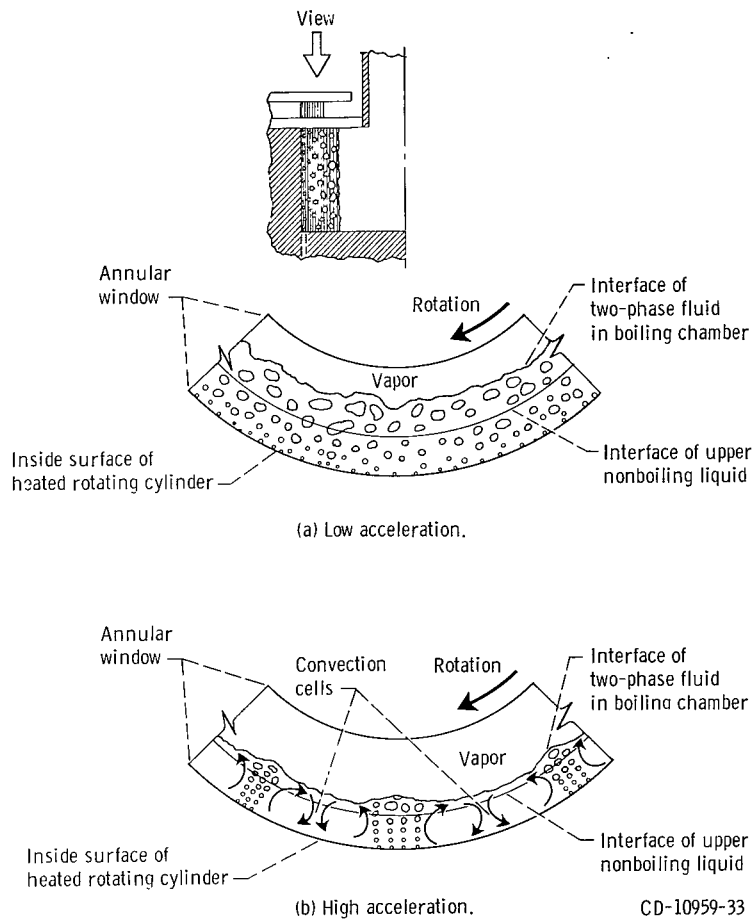


Figure 5. - Sketch showing typical views through top annular window at two accelerations and same heat flux.

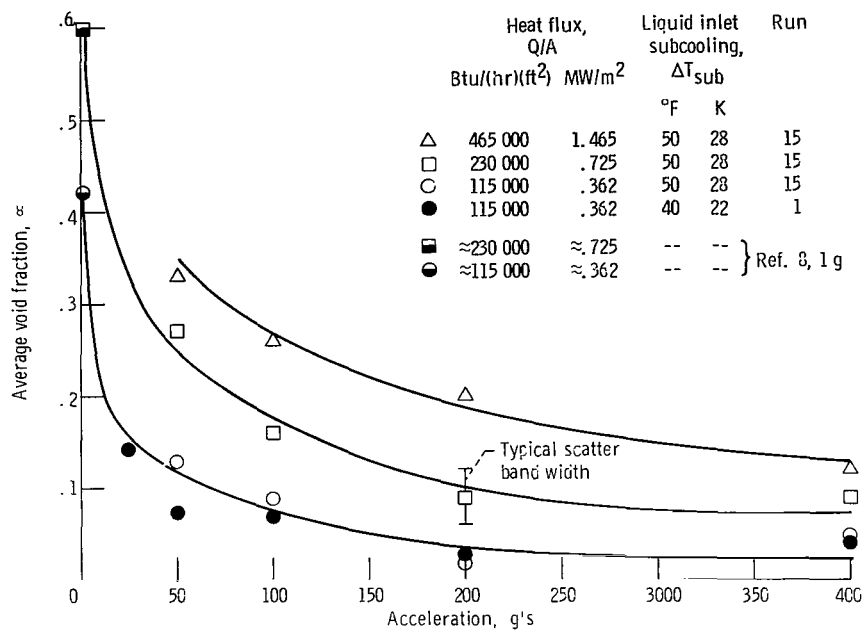


Figure 6. - Average void fraction of two-phase boiling annulus.

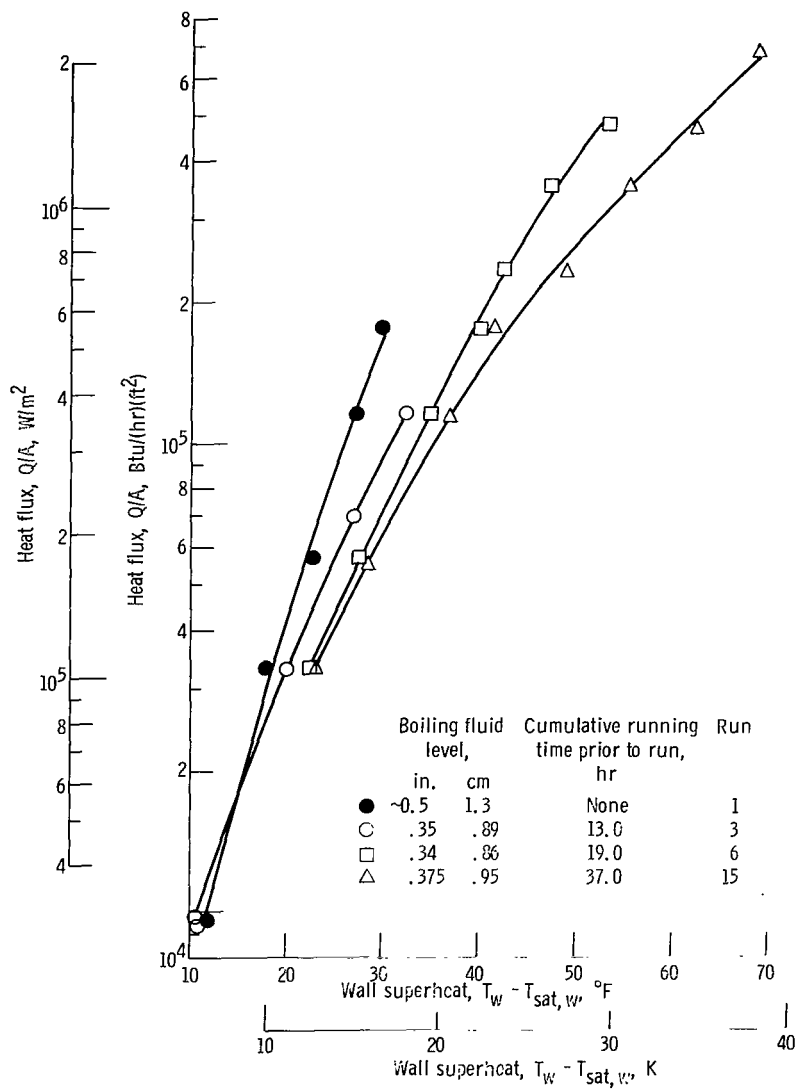


Figure 7. - Effect of test surface aging on 200-g nucleate-boiling data.

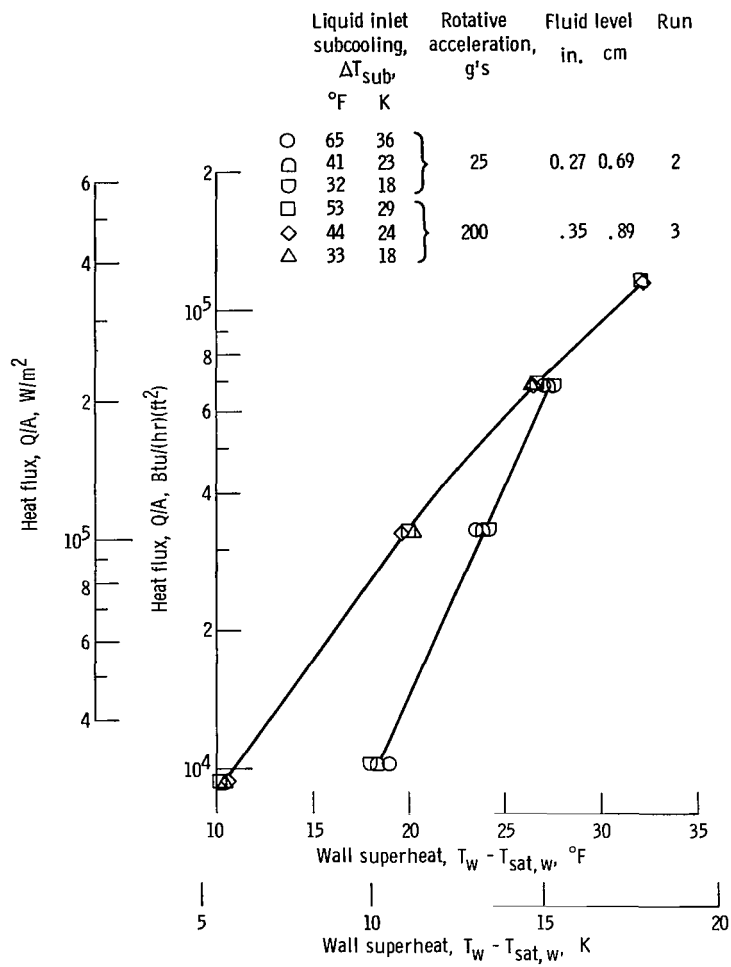


Figure 8. - Effect of inlet liquid subcooling.

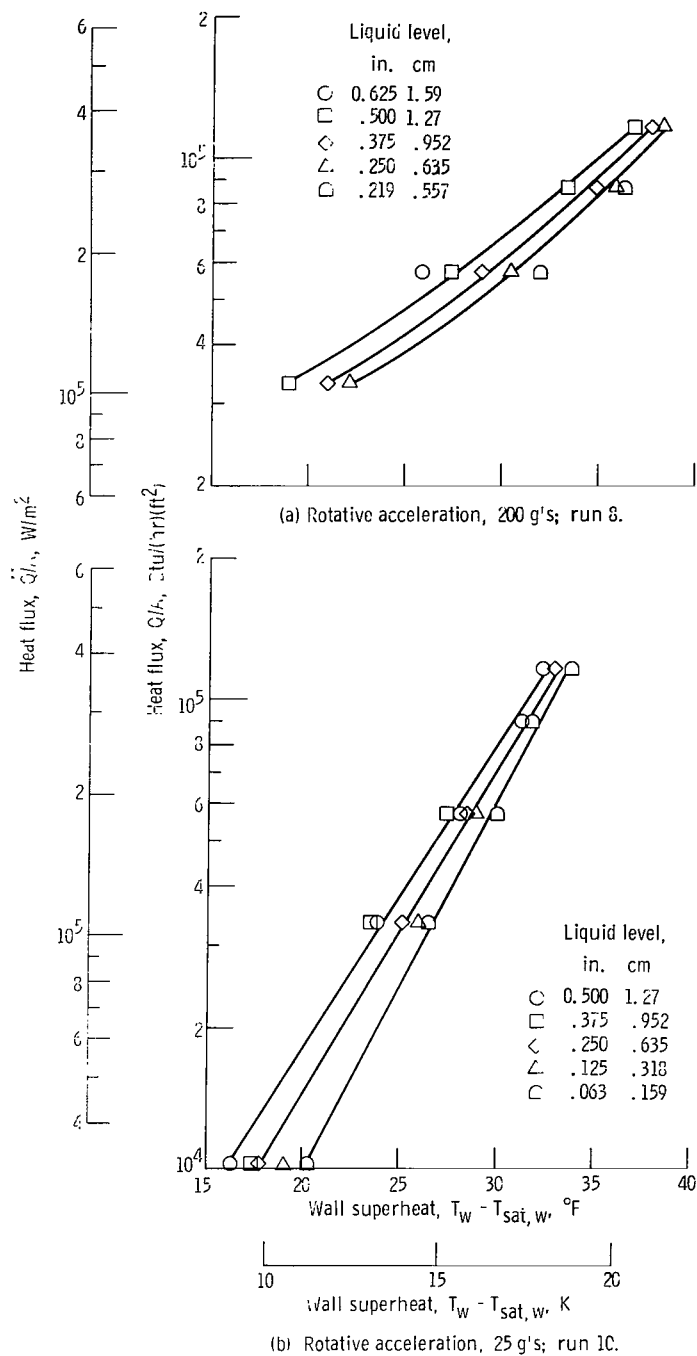


Figure 9. - Effect of liquid level (measured in top annulus) on boiling results. I.O inlet feed.

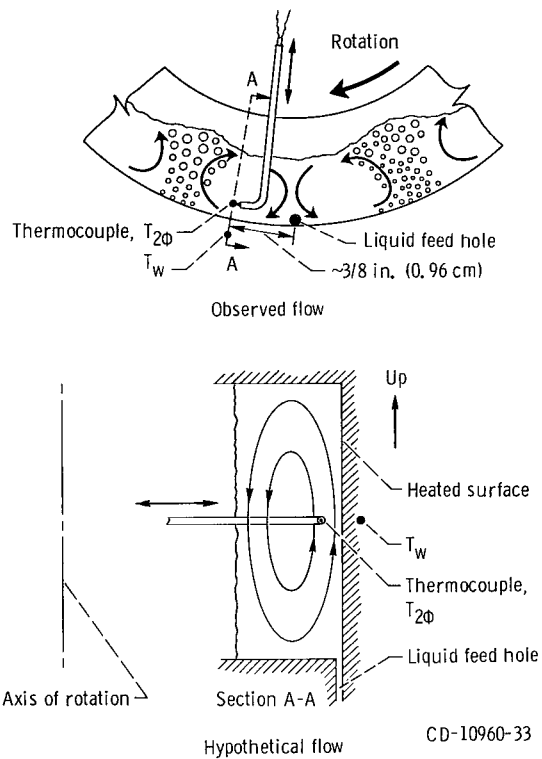
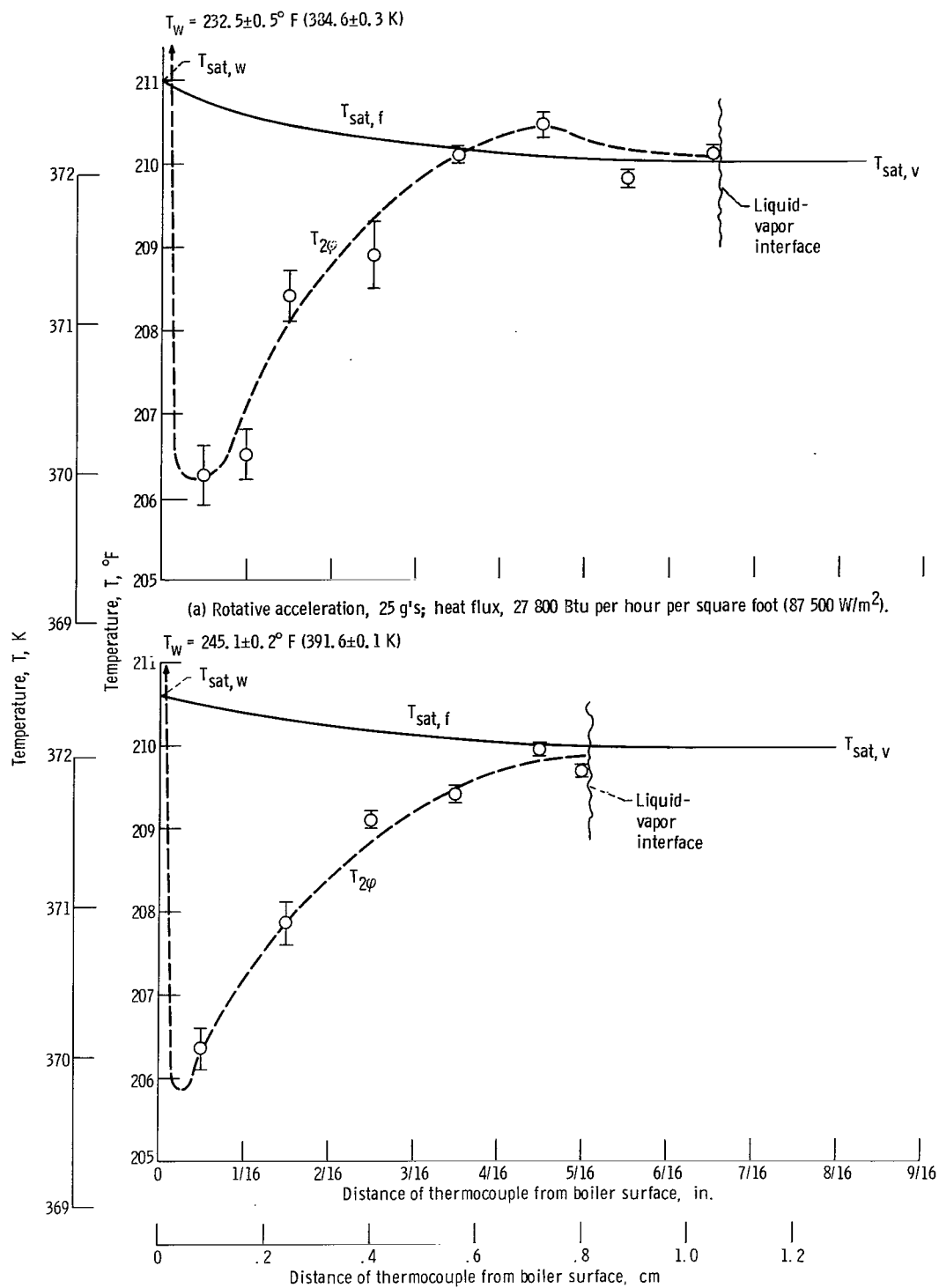


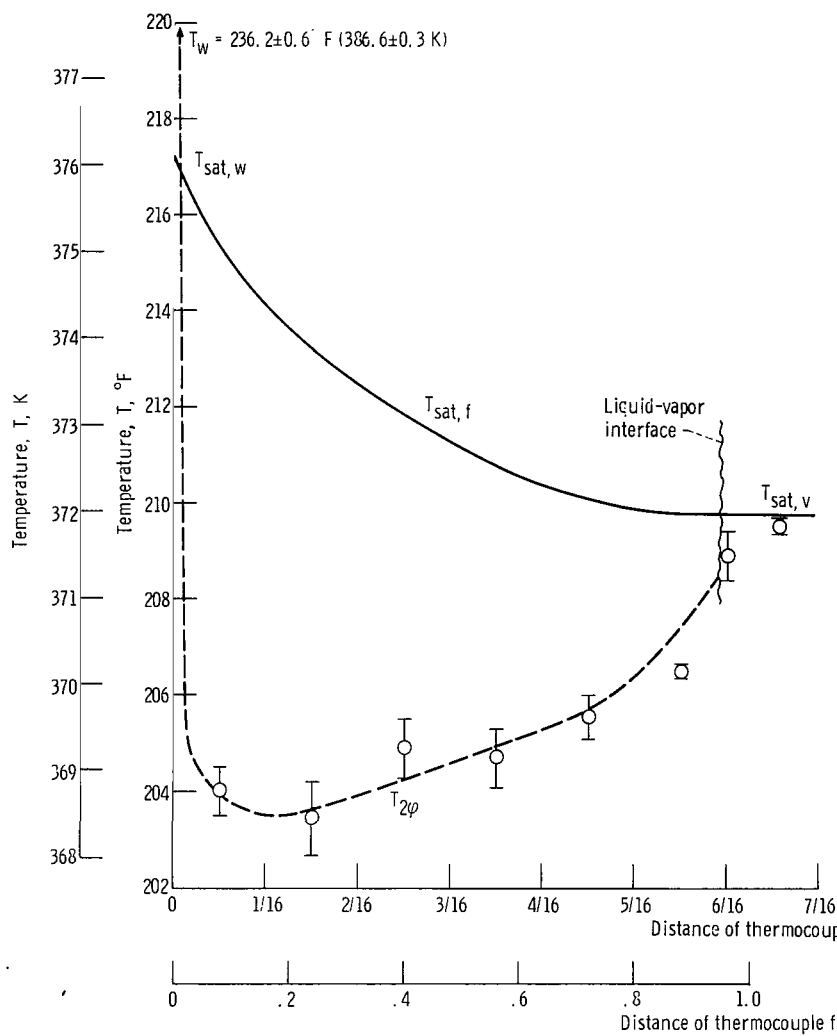
Figure 10. - Sketch showing position of thermocouple and flow pattern in two-phase fluid annulus.



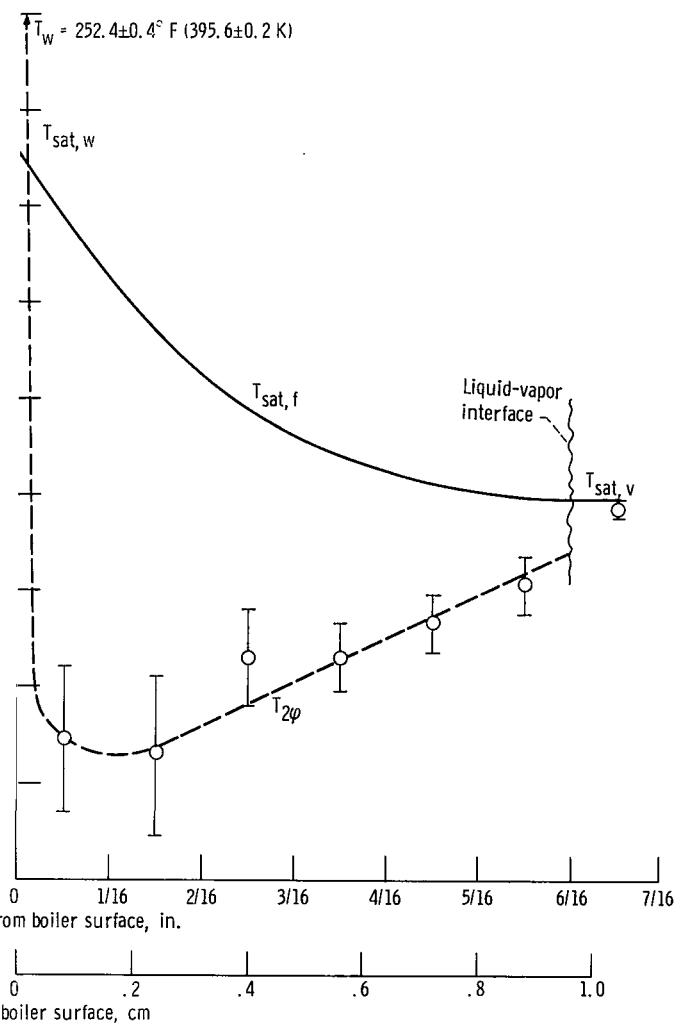
(a) Rotative acceleration, 25 g's; heat flux, 27 800 Btu per hour per square foot ($87\,500 \text{ W/m}^2$).

(b) Rotative acceleration, 25 g's; heat flux, 116 000 Btu per hour per square foot ($365\,000 \text{ W/m}^2$).

Figure 11. - Radial temperature profiles in two-phase fluid annulus. Run 13.



(c) Rotative acceleration, 200 g's; heat flux, 27 100 Btu per hour per square foot (85 200 W/m²).



(d) Rotative acceleration, 200 g's; heat flux, 115 000 Btu per hour per square foot (362 000 W/m²).

Figure 11. - Concluded.

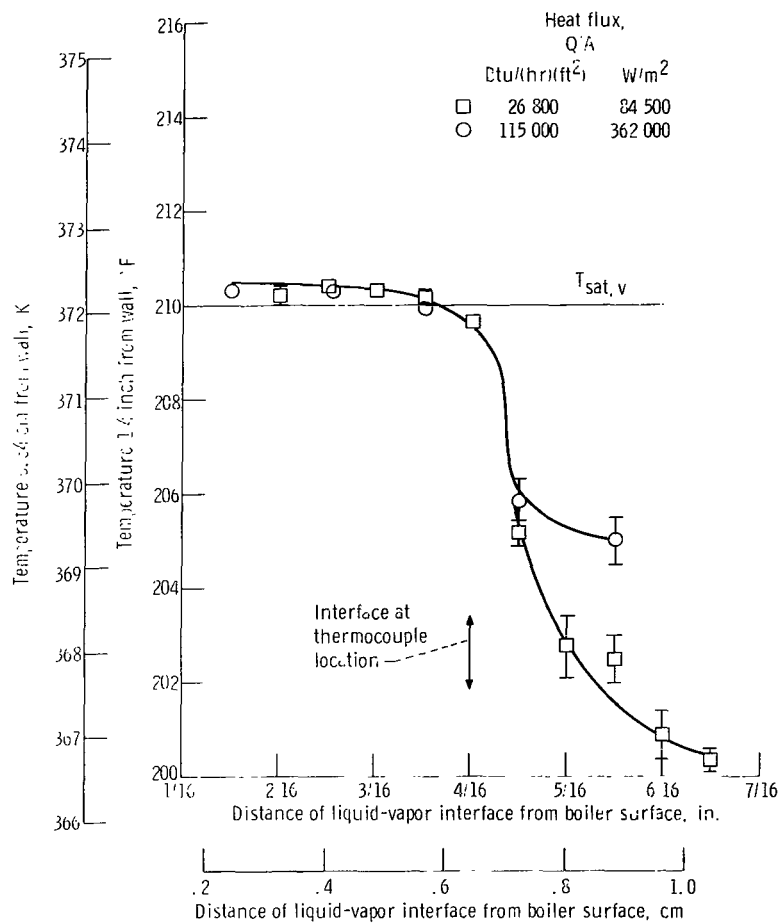


Figure 12. - Temperature 1.4-inch (0.64-cm) from boiler surface measured as fluid annulus thickness decreases. Run 14; rotative acceleration, 400 g's.

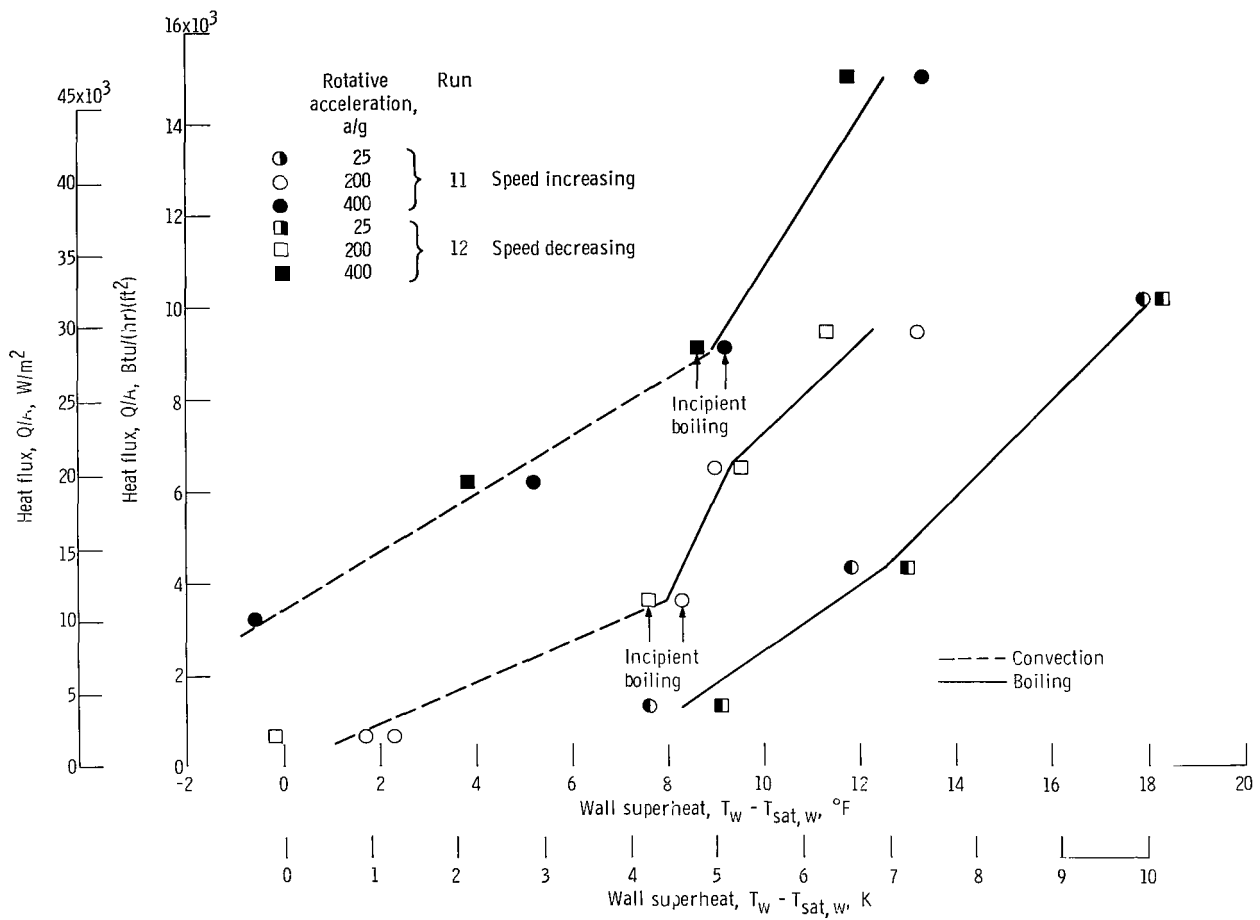


Figure 13. - Effect of acceleration on natural convection and incipient boiling.

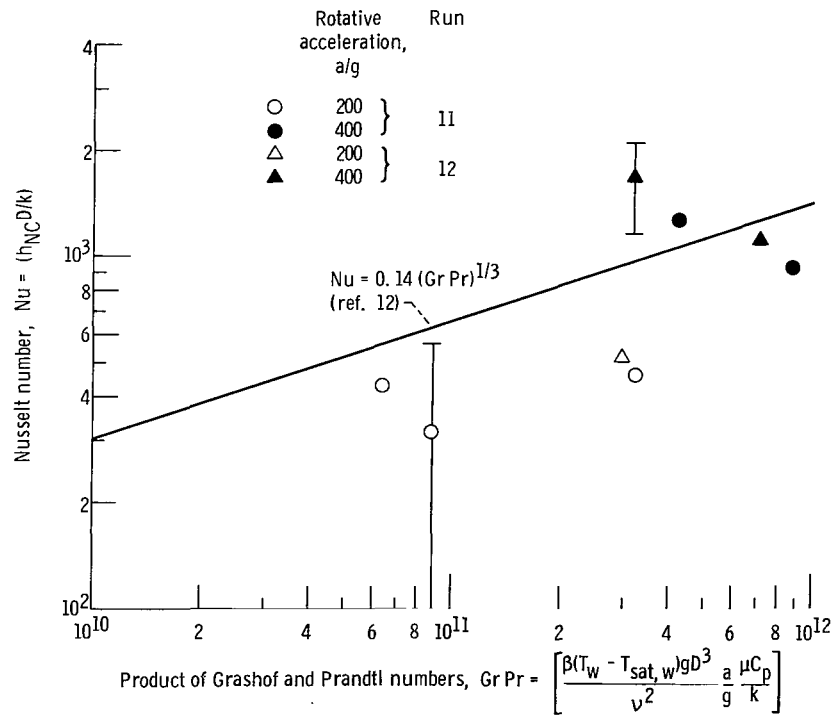


Figure 14. - Correlation of natural-convection data at or near boiling incipience.

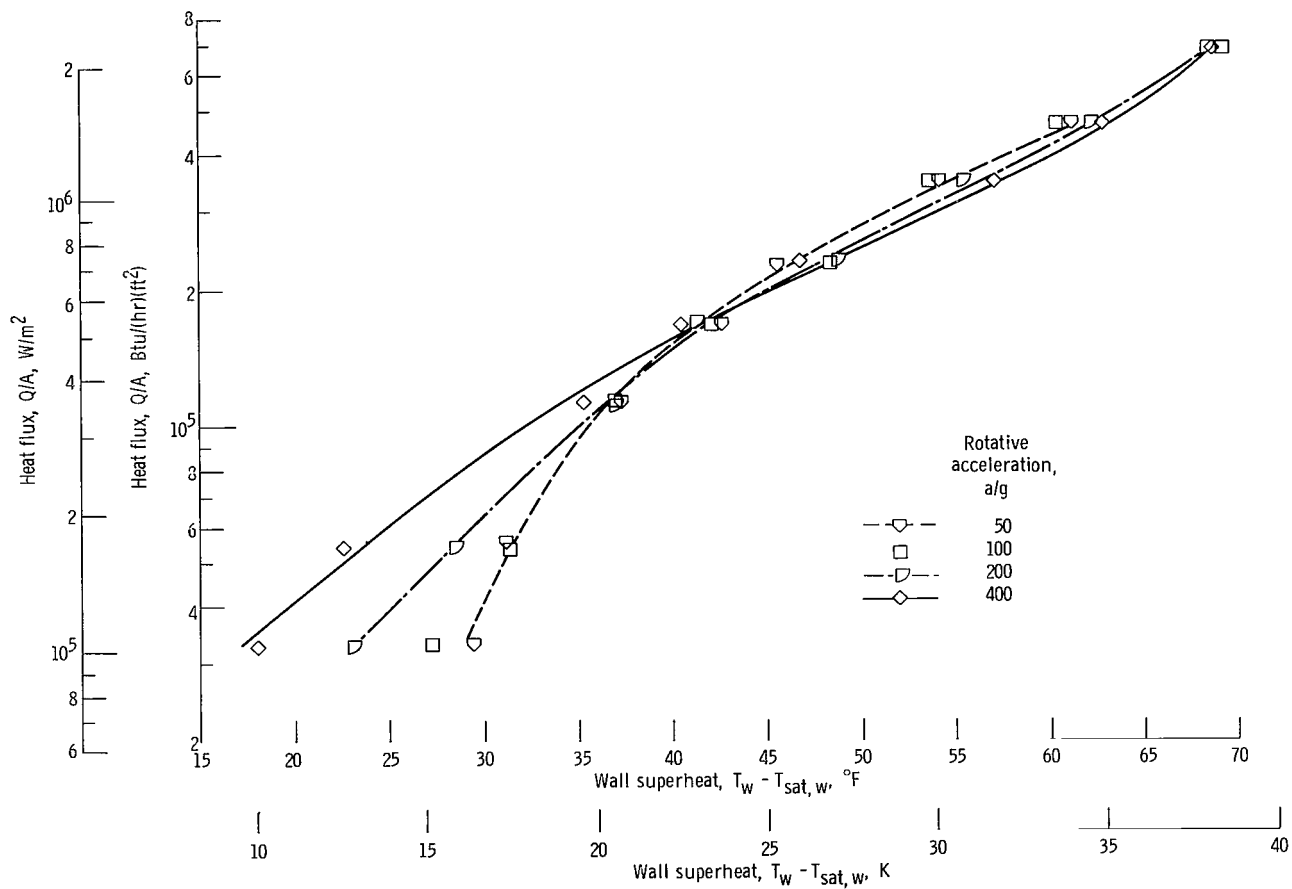


Figure 15. - Effect of acceleration on nucleate boiling; two-phase fluid level constant at 0.375 inch (0.95 cm). Run 15; liquid inlet subcooling, $\approx 50^{\circ}F$ (28 K).

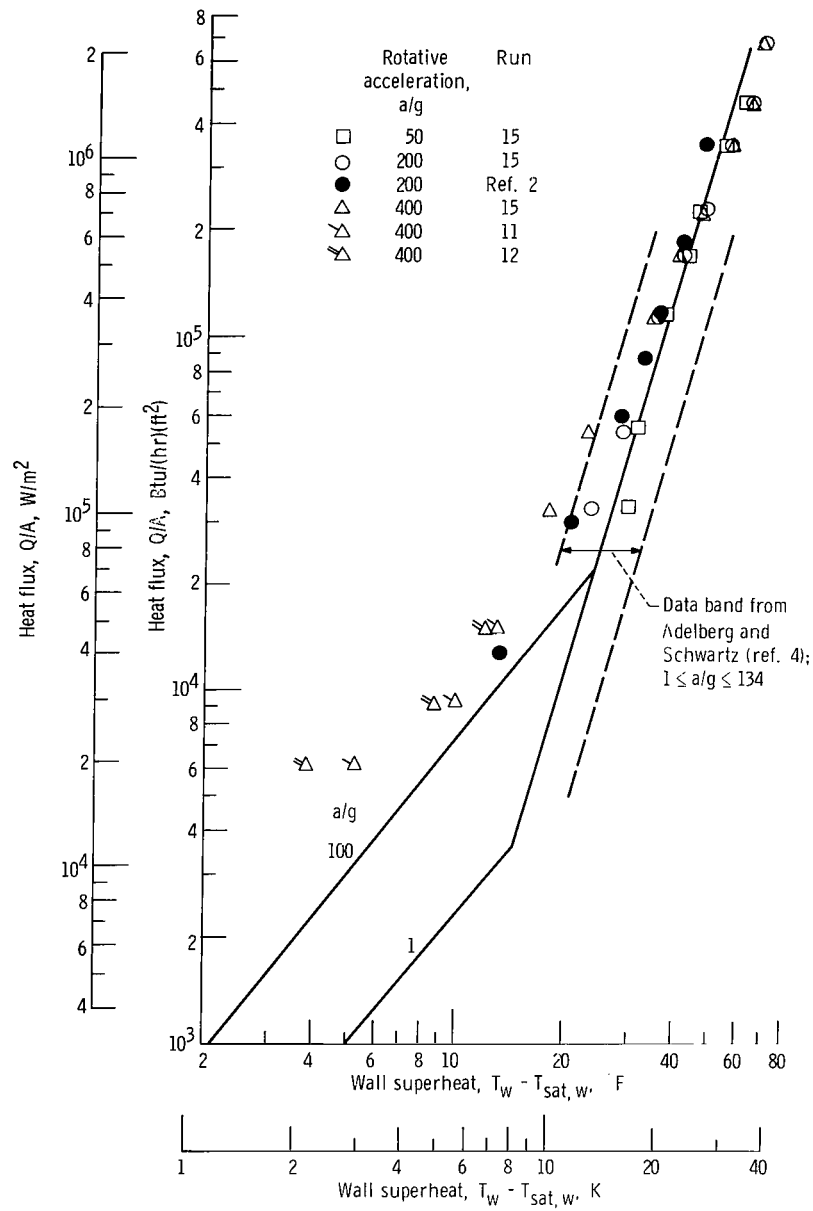


Figure 16. - Comparison of nucleate-boiling data at high accelerations.

NATIONAL AERONAUTICS AND SPACE ADMINISTRATION

WASHINGTON, D. C. 20546

OFFICIAL BUSINESS

PENALTY FOR PRIVATE USE \$300

FIRST CLASS MAIL



POSTAGE AND FEES PAID
NATIONAL AERONAUTICS AND
SPACE ADMINISTRATION

07U 001 58 51 3DS 71.10 00903
AIR FORCE WEAPCNS LABORATORY /WL0L/
KIRTLAND AFB, NEW MEXICO 87117

ATT E. LOU BOWMAN, CHIEF, TECH. LIBRARY

POSTMASTER: If Undeliverable (Section 158
Postal Manual) Do Not Return

"The aeronautical and space activities of the United States shall be conducted so as to contribute . . . to the expansion of human knowledge of phenomena in the atmosphere and space. The Administration shall provide for the widest practicable and appropriate dissemination of information concerning its activities and the results thereof."

— NATIONAL AERONAUTICS AND SPACE ACT OF 1958

NASA SCIENTIFIC AND TECHNICAL PUBLICATIONS

TECHNICAL REPORTS: Scientific and technical information considered important, complete, and a lasting contribution to existing knowledge.

TECHNICAL NOTES: Information less broad in scope but nevertheless of importance as a contribution to existing knowledge.

TECHNICAL MEMORANDUMS: Information receiving limited distribution because of preliminary data, security classification, or other reasons.

CONTRACTOR REPORTS: Scientific and technical information generated under a NASA contract or grant and considered an important contribution to existing knowledge.

TECHNICAL TRANSLATIONS: Information published in a foreign language considered to merit NASA distribution in English.

SPECIAL PUBLICATIONS: Information derived from or of value to NASA activities. Publications include conference proceedings, monographs, data compilations, handbooks, sourcebooks, and special bibliographies.

TECHNOLOGY UTILIZATION PUBLICATIONS: Information on technology used by NASA that may be of particular interest in commercial and other non-aerospace applications. Publications include Tech Briefs, Technology Utilization Reports and Technology Surveys.

Details on the availability of these publications may be obtained from:

SCIENTIFIC AND TECHNICAL INFORMATION OFFICE

NATIONAL AERONAUTICS AND SPACE ADMINISTRATION

Washington, D.C. 20546